Structures Research Report No. BB-512
FINAL PROJECT REPORT

March, 2000

UF Project No. 4910 4504 618 12
State Job No. 99700-3592-119
Contract No. BB-512
WPI No. 0510836

USE OF GROUT PADS FOR SIGN AND LIGHTING STRUCTURES PART 2 – CORROSION STUDY

Principal Investigators: Ronald A. Cook, Ph.D., P.E.
Mang Tia, Ph.D., P.E.

Graduate Research Assistants: Kevin B. Fischer
Daniel D. Darku

Project Manager: Marcus H. Ansley, P.E.

Department of Civil Engineering
College of Engineering
University of Florida
Gainesville, Florida 32611

Engineering and Industrial Experiment Station

STATE OF FLORIDA
DEPARTMENT OF TRANSPORTATION

UNIVERSITY OF FLORIDA
CIVIL ENGINEERING

USE OF GROUT PADS FOR SIGN AND LIGHTING STRUCTURES

State Job No. 99700-3592-119
Contract No. BB-512
WPI No. 0510836
UF No. 4910 4504 618 12

Principal Investigators:	R. A. Cook M. Tia
Graduate Research Assistants:	K. B. Fischer D. D. Darku
FDOT Technical Coordinator:	M. H. Ansley

Engineering and Industrial Experiment Station
Department of Civil Engineering
University of Florida
Gainesville, Florida

USE OF GROUT PADS FOR SIGN AND LIGHTING STRUCTURES
PART 2 – CORROSION STUDY

TECHNICAL SUMMARY

The goal of this part of the study was to investigate the effects of the use of grout pads on the corrosion resistance of the base plates for sign and lighting structures. Three different test specimens were constructed to replicate the base plate arrangements in the field - one with a grout pad of grout of low water permeability, a second one with a grout of higher permeability, and a third one without any grout pad. Two replicates of each of the test specimens were made. These specimens were subjected to daily wet-dry cycles in a 3.5% salt solution for 14 weeks to simulate a severe corrosion environment in the field. During this period, the corrosion of the embedded bolts and nuts were electrochemically monitored every two weeks using a linear polarization resistance technique with a guard ring electrode configuration. Visual observations were made of the embedded bolts, nuts and the base plates at the end of the wet-dry cycles. Weight loss measurements were also made.

The results of the electrochemical corrosion measurements did not show any clear trends with regards to the effects of grout pads. It is thought that the zinc coated base plates, which were used in the testing program, interfered with the electrochemical measurements.

The visual assessment and weight loss measurements showed that the use of grout pads under the base plates clearly improved the durability of the base plate arrangements. There was substantial rust observed on the anchor bolts in the base plate arrangement without a grout pad, while there was no discernible rust on the anchor bolts in the base plates with grout pads (see Figures 5.11 through 5.13). There was more deposition of white zinc oxide on the base plate in the arrangement without a grout pad than those observed on the two base plates from the arrangements with grout pads (see Figures 5.14 through 5.16). The average weight loss of the 16 bolts from the base plate arrangements without a grout pad was 0.628 g, while the average weight losses of the bolts from those with grout pads were 0.044 g and 0.063 g for Grout A (of higher permeability) and Grout B (of lower permeability), respectively. The weight loss of the bolts from the base plate arrangements without grout pads was significantly greater than those with grout pads. There is no significant statistical difference between the two grouts tested. It is thus concluded that the use of grout pads could improve the corrosion resistance of the base plates for sign and lighting structures.

TABLE OF CONTENTS

LIST OF TABLES

LIST OF FIGURES

CHAPTER 1
INTRODUCTION

1.1 The Problem

Tubular high mast poles, roadway light poles, and traffic mast arms are typically connected to a concrete foundation by an annular base plate and anchor bolts using double nut installation. In the design of these structures, both strength and serviceability requirements are of concern. Serviceability requirements are typically related to the control of deflections for the structure and long term durability.

Currently, the Florida Department of Transportation (FDOT) requires a grout pad beneath all signing and lighting structure base plates. Several states are eliminating this as a requirement believing that it is detrimental to the maintenance inspections of the structures.

Based on recent failures during Hurricane Opal, there is evidence that these pads are essential to the performance of these structures. Figure 1.1 shows the schematic diagram of typical components in this type of installation while Figures 1.2 and 1.3 show a picture of a base plate of a lighting post installed with a grout pad and a picture of a lighting post in service, respectively.

1.2 Project Objective

The objectives of this research were:

(1) to acquire sufficient data to investigate the corrosion of the base plate arrangement,

(2) to make comparison of the corrosion of embedded bolts and nuts of the base plate arrangements with and without grouts, and

(3) to propose recommendations for the use of grout pads under base plates for lighting and signing posts.

1.3 Scope of Investigation

The following testing programs were performed:

(1) Water absorption tests were performed on the grouts which have been certified for use by the FDOT. The results of these tests can serve as the basis for comparison of the relative corrosion protection of the grout to the embedded metals in the grouted arrangements since results of various prior research studies (1) have established that the durability of concrete structures depend greatly on permeability and water absorption of the concrete.

(2) Accelerated corrosion tests (cyclic immersion in 3.5% salt water) and subsequent corrosion rate measurements using the linear polarization resistance technique were carried out on samples fabricated to replicate the actual field arrangement of

base plates with and without grout.

(3) Visual assessment of the anchor bolts in the base plate arrangements was made at the end of the accelerated corrosion testing by cutting the grouts and exposing the embedded anchor bolts. These visual assessments were used to confirm the electrochemical measurements .

(4) Weight loss measurements due to corrosion were made by weighing the embedded nuts within the arrangements with the rust after the wet - dry cycling . The nuts were then cleaned of rust using wire brush and the weight taken again to obtain the weight loss due to corrosion.

The results of the corrosion tests were analyzed and compared with those of the water absorption tests to determine if absorption of the grouts has an effect on the corrosion resistance of the anchor bolts of the sign and lighting structures. This will assist in the selection of grouts for such installations.

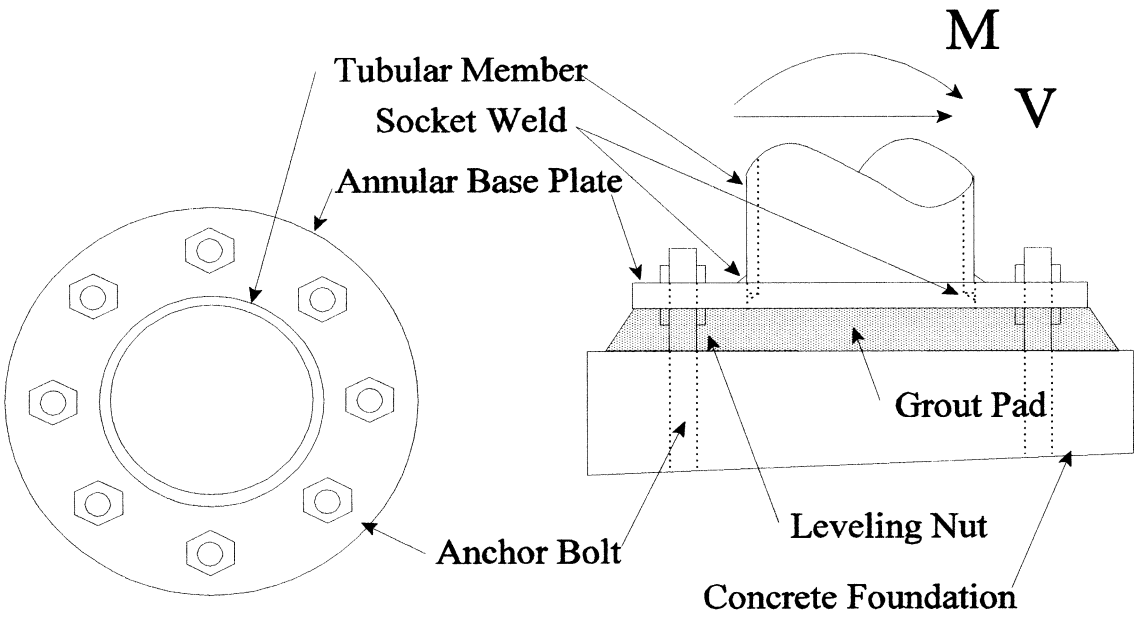

Figure 1.1 : Typical Components of Installation

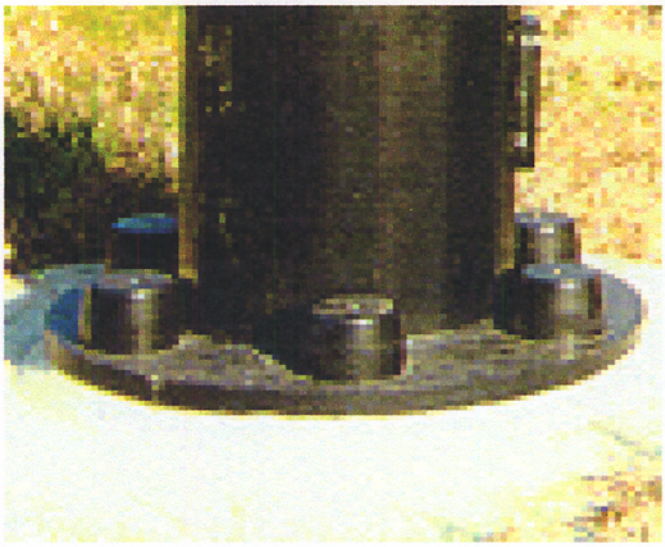

Figure 1.2: Installed Sign Pole With Grout

Figure 1.3: A Typical Lighting Installation in Service

CHAPTER 2
LITERATURE REVIEW

2.1 Introduction

Tubular high- mast poles, roadway poles, and traffic mast arms are typically connected to a concrete foundation by an annular base plate and anchor bolts using a double-nut installation. A socket weld forms the connection between the annular base plate and tubular member. These types of structures are subjected to relatively high bending moments with some shear accompanied by relatively small axial compression loading when an external force, which are usually strong winds as frequently experienced in Florida from hurricanes and during thunder storms.

A recently completed FDOT research project (2) revealed that the total deflection of these structures comprised of the deflection caused by the tubular member plus deflection caused by the rotation of the base of the structure.

The rotation of the base of the structure comes from the flexibility of the anchor bolts, the base plate, and the socket welded joint. Further research (3) showed that a significant amount of the overall base rotation was due to the elongation (tension side) and shortening (compression side) of the anchor bolts.

The use of grout pads under the base plates will provide additional support under the base plate on the compression side, but insignificant change on the tension side.

This may tend to decrease the overall base rotation. The structural effect of the base plate arrangement with a grout pad is the subject of a parallel research. This project is primarily concerned with the durability of the grouted base plate arrangement.

2.2 Cementitious Grouts for Machine and Structural Steel Bases

Various materials are used for grouting, depending on the function the grout is expected to perform. They may range from plastic mortars, thick , semi liquid (flowable) or liquid (fluid) suspension of cement and other compounds and additives in water. Solution of chemicals, resins, artificial foams, hot bitumen and bitumen emulsion may also be used in some cases .

For grouting of machinery bases and bases for structural steel , cementitious grouts are used for their stability, durability and strength properties, especially in the case of this project where the structures are exposed to the vagaries of the weather (extreme heat and cold, rain, snow) and where the grout is required to enhance the structural performance of the base plate arrangement.

Cementitious grouts are usually a suspension of cement , fine aggregates and additives for stability in water. Grouts for machine bases and bases of structural members must have the following properties;

a) Stability of the suspension to avoid bleeding.

b) The suspension must have the required consistency to ensure that it can be placed to fill the space under the base plates while at the same time maintaining the physical properties necessary to achieve durability and strength requirements.

c) Strength gain with time as well as the ultimate strength of the grout must be such that the grout should be able to perform the required structural function. Most manufacturers specify the strength and setting times as a guide to users.

d) Resistance to corrosion of the grout material is critical for the durability of the base plate arrangement when water which is chemically aggressive to Portland cement and embedded metals is to come into contact with the setup. Chemically aggressive waters may be in the form of acid rain which are predominant in heavy industrial settings (e.g the Tampa Bay) or saline water near the coast as is predominant in the numerous coastal towns dotted along Florida's coast. Although the permeability of most grouts is low, after a long period of exposure substantial deterioration of embedded metals in the grout may occur through corrosion.

e) Volume stability of the grout is of importance as the shrinkage of the set grout could lead to a deficiency in the structural performance of the grout by creating a gap between the grout and base plate.

Ordinary plastic and fluid mortars are inadequate to perform the above functions due to the inherent tendency of solid constituents to settle and leave a layer of water at the top (bleeding) and drying shrinkage which reduces the volume when dry. Stable non - settling grout mixes can be prepared by a prolonged delayed mixing or by adding a special ingredient to ordinary mortar. Akthem A. et. al.(4) , have indicated that the use of condensed silica fume and superplasticizer produces very stable grouts.

Silica fume has been found to decrease the porosity (5) and hence fluid transport (6,7) through the grout and subsequently increases its strength and durability. Superplasticizer helps produce flowable mix at low water - cementitious materials ratio which enhances both the physical and chemical properties of the grout.

2.3 Durability of Steel Embedded In Grout Pads

Problems of steel durability are manifested by deterioration of the grout either by external factors or internal causes within the grout. Durability of the embedded metals within the grouts is influenced by the ease of transport of fluids through the grout since the transport of external fluids within the grouts affects the corrosion of the embedded bolts and nuts as water, oxygen , chlorides and carbon dioxide can easily access the metal and either initiate or enhance corrosion which will subsequently reduce the effectiveness of the bolts .

2.4 Basic Corrosion Mechanism

Metallic corrosion is usually an electrochemical process. Electrochemical processes require anodes and cathodes in electrical contact and an ionic conducting path through an electrolyte. The electrochemical process includes an electron flow between the anodic and cathodic areas, which quantify the rates of the oxidation and reduction reactions that occur at the surfaces. Monitoring this electron flow (corrosion current) provides the capability of assessing the kinetics of the corrosion process as well as the thermodynamic tendencies and mass loss.

2.4.1 Electrochemistry of Aqueous Corrosion

The surface of a corroding metal behaves as a mixed electrode on which coupled anodic and cathodic reactions take place. Metal atoms pass into solution as positively charged hydrated ions (anodic oxidation). Excess free electrons from here flow through the metal to the cathode where they are accepted by either hydrogen ions or dissolved oxygen (cathodic reduction). The process is completed by electron migration between anodic and cathodic sites through the aqueous phase, leading to the formation of a corrosive product.

2.4.2 Electrode Potentials

The flow of current (electrons) between the local anodic and cathodic sites on the metal implies that an electrical potential difference must exist between these sites. Figure 2.1 illustrates the corrosion of iron in oxygenated water.

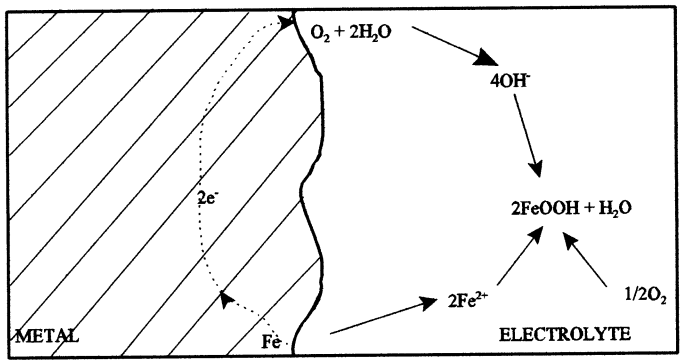

Figure 2.1 Corrosion of Iron in Oxygenated Water

If ϕ_m and ϕ_s are the free potentials at the metal phase and solution phase respectively, the potential drop (ϕ_m - ϕ_s), which represents the drop across the electrical double layer, is called the electrode potential, denoted by (E). The net potential at the local anode (ϕ_m^a - ϕ_s^a), across the electrical double layer is always less than that at the cathode (ϕ_m^c - ϕ_s^c) (11). The difference between the two electrode potentials may be negligible if the anodes and cathodes are closely spaced and the electrolyte solution is of high conductivity , but may be significant (several hundreds of millivolts) if anodes and cathodes are separated by a medium of high resistance such as concrete.

Relative values of electrode potentials are measured in reference to scales for which the zero point is arbitrarily defined by the fixed electrode potential of some reference half cell (Standard Hydrogen Electrode (SHE), Copper Sulphate Electrode (CSE) or Standard Calomel Electrode(SCE)).

Thermodynamically (11), corrosion reaction will only be feasible if the potential of the electrode system (E) is less than the potential at the equilibrium state (E_o). Thus if E_o for a particular electrochemical reaction is known, it is possible to predict the range of electrode potentials over which the reaction will be thermodynamically feasible at any given concentration of the reactants and products.

2.4.3 Electrochemical Polarization

In the equilibrium state, the rates of the reversible anodic and cathodic processes , represented by i_a and i_c respectively are equal and opposite and the net measurable current is zero.

$i_a = | i_c | = i_o$

i_o is referred to as the exchange current density for the reaction.

If E is greater than E_o, then the anodic process is favored, i.e $i_a > | i_c |$ and if $E<E_o$, the cathodic process dominates and $i_a < | i_c |$. In either case, the electrode is said to be polarized and the driving force for the reaction, $(E - E_o)$, is related to its overpotential. In an electrolytic cell arrangement in which the metal under investigation (the working electrode) has its electrode potential controlled by a potentiostat, the resulting graph of $(E - E_o)$ versus the current (i) or log of it are known as the Polarization curves as shown in fig 2.2.

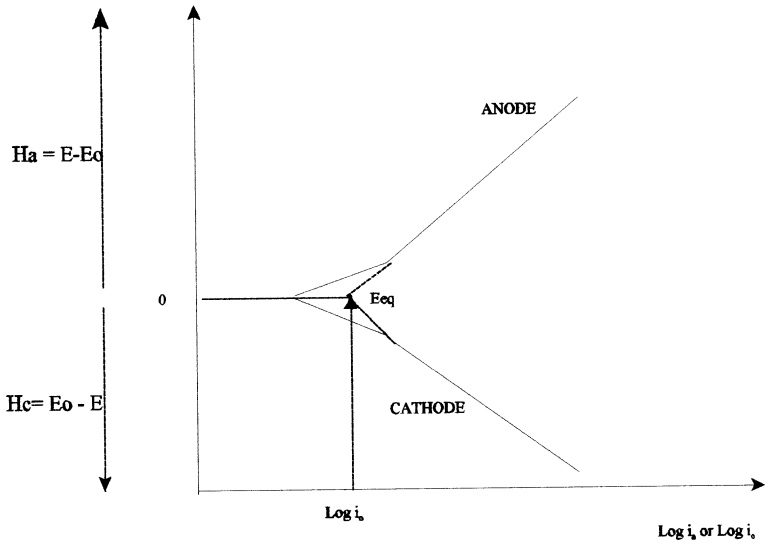

Figure 2.2: Polarization curve for an electrode process (Known as the Tafel Plot)

The relationship between overpotential (E -Eo) and current density is known as the Tafel Equation. For corrosion in the absence of externally applied potential, the oxidation of the metal and the reduction of some species in solution occur simultaneously at the metal/electrolyte interface.

2.4.4 Microcell Corrosion

A single polarized anodic reaction ($Fe - 2e^- = Fe^{2+}$) and a single polarized cathodic reaction ($O_2 + 4e^- = 2O^{2-}$) are coupled to form numerous microcells on the surface of the metal immersed in an electrolyte of high conductivity. This is represented in the Evans diagram shown in figure 2.3

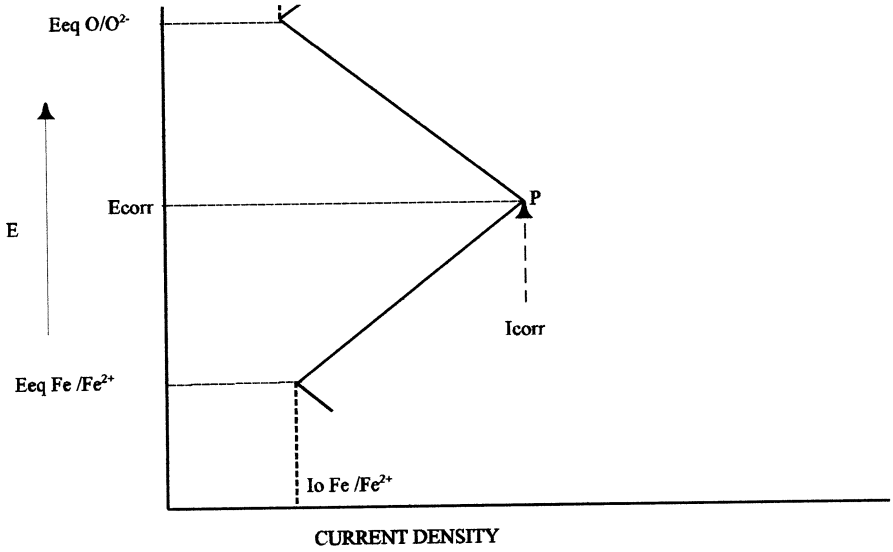

Figure 2.3: Evans Diagram for Simple Corrosion

At the point P, the mean anodic and cathodic current densities are equal and represent the corrosion rate in terms of a mean corrosion current density (Icorr). The electrode potential of the couple at this point is termed the corrosion potential (Ecorr).

2.4.5 Ohmic Drop

In practice, there is always some difference between the electrode potentials developed at anodic and cathodic sites on the metal surface. This difference is negligible when corrosion takes the form of microcell action, but in the case where the anodic and cathodic areas are separated by a medium of high electrolytic resistance (Macrocell corrosion), a significant ohmic drop exists which affects the corrosion potential. The mean corrosion rate is significantly reduced in this case. Figure 2.4 illustrates this.

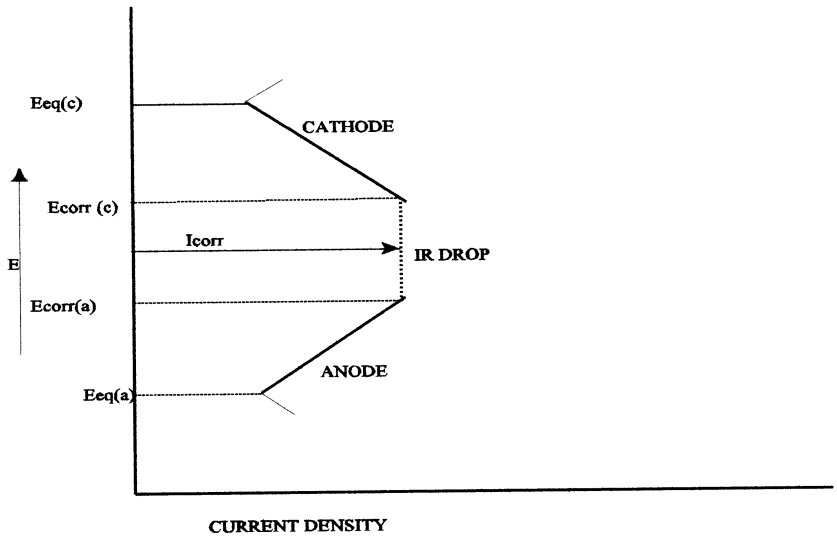

Figure 2.4; Evans Diagram For Corrosion Couple With Ohmic Drop

2.5 Corrosion of Steel in Cementitious Medium

Concrete, mortars and grouts contain microscopic pores with high concentration of soluble calcium, sodium and potassium hydroxides which are very soluble in water. The presence of this pore solution creates a very alkaline environment (PH well above 11). In the presence of oxygen, the alkaline pore solution, forms a passive layer on the surface of the embedded steel.

The establishment and maintenance of this film forms a physical and chemical barrier against the penetration of deleterious substances, prevent access of water and oxygen from reaching the metal surface and therefore prevents the corrosion of embedded steel in concrete, mortar or grouts. The layer is probably part metal oxide or hydroxide and part mineral from the cement (5). Maintenance of passivation is conditional on an adequately high pH value of the pore water in contact with the passivating layer.

Corrosion is initiated when the passive layer breaks as water and oxygen reaches the steel surface. Two processes known to break the passive layer (referred to as depassivation) are carbonation and chloride attack.

2.5.1 Carbonation

Carbon dioxide from the atmosphere forms a weak carbonic acid either when it is in contact with the pore solution within the grout or in the form of acid rain which directly penetrates the grout and reduces the pH to a value of about 9.0 by reacting with calcium hydroxide ($Ca(OH)_2$ in the hydrated lime in the following reactions;

$$CO_2 + H_2O \rightarrow H_2CO_3$$

$$H_2CO_3 + Ca(OH)_2 \rightarrow CaCO_3 + 2\,H_2O$$

When all the $Ca(OH)_2$ is carbonated, the pH value is reduced to 8.3 (6). This removes the protective oxide layer and initiates corrosion.

2.5.2 Chloride Attack

Chlorides act as catalysts to corrosion at sufficient concentration at the rebar surface to break down the passive layer. There is no overall pH drop in this case. Chlorine is not consumed in the process but helps to break down the passive layer on the steel and allows the corrosion process to proceed quickly. Hausermann (5) observed that when the chloride concentration exceeds 0.6 of the hydroxyl concentration, corrosion is observed. This approximates to a concentration of 0.4% chloride by weight of cement if chlorides are cast into concrete and 0.2% if they diffuse into it.

The chloride depassivation reaction is given by the following equation;

$$2Fe_2O_3 + 8Cl^- \rightarrow 4FeCl_2 + 3O_2$$

The passive oxide (Fe_2O_3) is broken down and at the same time oxygen is released which promotes the corrosion of the embedded steel. Chloride is further released into solution as follows;

$$FeCl_2 \rightarrow Fe^{2+} + 2Cl^-$$

The corrosion state is characterized by galvanic action between relatively large areas of passive steel acting as cathode and small anodic pits where the local environment, within the pits, develops a high chloride concentration and a depressed pH value (pitting).

It is however necessary that a sufficient concentration of oxygen be present to cause polarization of the anode to potentials more noble than the breakdown potential characteristics of the embedded steel.

General corrosion may also be observed when the grout has become contaminated with chloride ions to such an excessive level as to cause virtually complete destruction of the passive film. Note must be made however that in very dry concrete, corrosion may not occur even at very high chloride concentration as water is not present.

2.5.3 Electrochemistry of Corrosion of Steel in Concrete

The corrosion potential of steel in its normal, protected state in sound concrete may vary over a wide range , from about +200mV to -700mV(SCE scale) or (+130mV to -800mV (CSE scale)), depending on the availability of the cathode reactant, namely oxygen. For reinforced concrete exposed to air, the level of dissolved oxygen will be sufficient to maintain the corrosion potential of passive steel in the range of + 30mV to -270mV (SCE) (11). The quality of the concrete and thickness of cover to the embedded steel both affect the stability of the passive state by excluding aggressive substances.

The average corrosion potential of steel reinforcement undergoing pitting is likely to be in the range of -200mV to -500mV (SCE) or -200mV to -570mV (CSE) (11). The corrosion potential of reinforcement undergoing general corrosion is usually in the range of -450mV to -600mV (SCE) or -520 to - 670mV (CSE), similar to that of steel undergoing corrosion in a nearly neutral aqueous environment.

In environments where oxygen is depleted or extremely limited, as in fully submerged or buried concrete, the metal undergoes uniform dissolution to form soluble $FeOH^-$ ions. The corrosion potential is depressed to values in the approximate range of -700 mV to -1100 (CSE) or -770 mV to -1100 mV (CSE) or more negative and the rate of metal dissolution is extremely low owing to the restricted availability of cathode

reactants. In practice, such low potentials will rarely be reached in the grouted base plate arrangement for lighting and signing structures.

2.5.4 Atmospheric Corrosion

The arrangement of base plates exposes the upper parts of the steel bolts and nuts to atmospheric corrosion. Atmospheric corrosion takes place only during the time when the metal is wet with liquid moisture. Dew is an important contribution to the formation of surface moisture films. Surface wetness occurs when a critical relative humidity (RH) is exceeded.

In the presence of acidifying pollutants such as SO_2 in heavy industrial settings, the anode reaction is facilitated and consequently, the total corrosion rate is increased. Deposition of chlorides from deicing salts and from marine droplets also increases corrosion rates as explained earlier (acts as depolarizers). With increasing moisture layer thickness, anode efficiency also increases and the electrolyte resistivity decreases. The reaction is then controlled by diffusion of O_2 molecules to the cathode.

Particles of dust may act as nuclei for moisture condensation and so influence the film thickness. Temperature affects both the corrosion rate and the dew point.

When steel is exposed to the atmosphere, the thickness of the electrolyte layer (water from dew or rain) determines the conditions for the development of the anodic and cathodic processes.

2.6 Modes of Fluid Transport Within Grouts

Pure water, or water carrying aggressive ions, carbon dioxide and oxygen can enter and move through the grout by diffusion, sorption, or permeation (flow under pressure). The nature of the pore system within the grout influences the entrance and subsequent movement of fluids through it.

2.6.1. Diffusion

Diffusion is the transfer of mass by random motion of free molecules or ions under a differential in concentration within the pore solution of the grout resulting in a net flow from areas of higher concentration to those of lower concentration. Oxygen, carbon dioxide and other gasses may move within the grout through this mode of fluid transport. However, their presence in the absence of water is of little significance as corrosion cannot proceed without the presence of water.

2.6.2 Sorption

Sorption is the capillary movement of fluids within the pores of the grout. This can take place only when the grout is totally or partially dry. There is no sorption of water in a completely saturated concrete. The condition of exposure of the base structure of lighting and signing posts do not normally allow for permanent submergence and hence the mode of contact with water is short and there is no pressure head developed to warrant fluid flow under pressure through the grout. Permeability is therefore not considered as the predominant mode in the arrangement. Capillary absorption is the primary mode of the ingress of chlorides and carbon dioxide into the grout.

The unsaturated grout pad in contact with a salt solution will take up the salt solution by capillarity forces. The chlorides are further transported by diffusion to increase the depth of penetration, however, the penetration by absorption is much faster. The absorption characteristics of the outer zone of the grout which offers the main protection to embedded metals is therefore of significance in this study.

2.6.3 Rate of Absorption

The initial absorption rate when a solid is in contact with a liquid for a short term is given by the equation;

$$a = (\Delta m) / (Af(t)) \text{----------} (2.1)$$

Where a = Absorption rate (g/m^2s^n)

Δm = weight of Liquid taken up

A = Area in contact with water

f(t) = Time function

f(t) is usually $t^{1/2}$ for most concretes and mortar (9). However, different time functions may be obtained for some concretes and mortars.

2.6.4 Relationship Between Sorption, Diffusion and Permeability.

Research results (7 and 8) have shown that the flow of liquids, gases and ions in a specific concrete or mortar are interrelated to a certain degree. The rates of diffusion and permeability were shown to increase with increasing absorption rate (sorptivity). Therefore, by estimating one of the modes of transport for different materials, the trends of fluid transport via the other modes can be perceived.

2.6.5 Absorption Rate Measurement

Water absorption into a sample from a water reservoir may be tested by means of three principally different set ups, (a) the horizontal case in which the water absorption rate is independent of gravitational effects, (b) the infiltration case in which the water percolates through the medium from top to bottom and the total flow is the sum of capillary- driven and gravitational driven flows and (c) the capillary rise case in which the effects of capillary and gravity are opposed (a capillary rise equilibrium is ultimately attained). For many building materials, water absorption rates measured in the three configurations are similar because capillary is dominant (9).

The set - up for the sorptivity test as proposed by Hall (9) and which is widely used is shown in Figure 2.5.

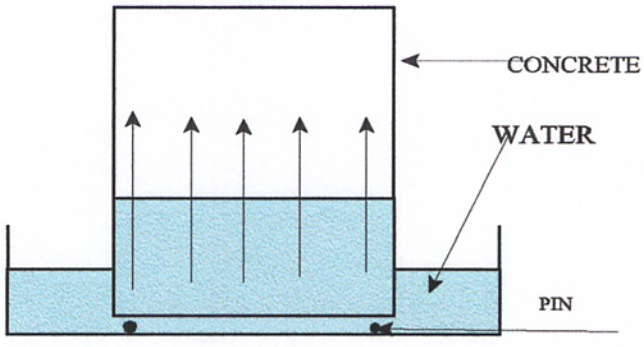

Figure 2. 5. Setup for The Absorption Test (Hall)

The lower parts of the sides of the samples adjoining the inflow face may be sealed with bituminous paint or other coating to prevent absorption. The specimen should rest on rods or pins to allow free access of water to the inflow surface. The water level should not be more than 5 mm above the base of the specimen. The quantity of water absorbed is measured at intervals by weighing the specimen. Surface water should be mopped off with a damp tissue. Each weighing should be completed within 30 seconds, and the timing device should not be stopped during weighing. A minimum of 5 points is necessary to define a good sorptivity plot.

Other proposed methods of absorption measurements, namely the Initial Surface Absorption Test (ISAT) (Described in British Standard 1881), the Figgs method (12) and subsequent variations even though applicable in the laboratory, does not offer any advantages over uniaxial flow (9).

2.6.6 Effect of Concrete Pore Saturation

On exposure to the atmosphere at a given relative humidity and temperature, the humidity contained in the pores of the concrete comes to equilibrium with the ambient humidity. The humidity of the atmosphere therefore determines the degree of saturation of the concrete pores and hence the corrosion of embedded metals.

When concrete is in contact with water for a long duration or in a moist room which is water saturated, all the concrete pores will be fully saturated and transfer of oxygen through the concrete pores to the reinforcement will take place exclusively through liquid phase diffusion.

W. Lopez and J. A. Gonzalez (13) observed that increased oxygen supply through concrete cover occurs at relative humidities of 60 - 70% which results in increased corrosion through triggering of the passivity - activity transition in the steel and local acidification at the steel/concrete interface. They also found out that below a practical critical pore saturation of 45 - 50%, corrosion risks are negligible for practical purposes.

2.7 Corrosion Rate Measuring Techniques

2.7.1 Electrochemical Methods

Many electrochemical methods of corrosion rate measurement have been developed, each providing specific information and having characteristic advantages and disadvantages. Three methods that have proved useful for evaluating the corrosion of rebars in concrete are the corrosion potential and potential mapping technique, the linear polarization resistance technique and electrochemical impedance spectroscopy (EIS) technique.

Generally, the measurements involves the determination of the amount of steel dissolving and forming oxide (rust) at the anode. This is done directly as a measurement of the electric current generated by the anodic reaction.

$$Fe \rightarrow Fe^{2+} + 2e^{-}$$

and consumed by the cathodic reaction:

$$H_2O + 1/2\ O_2 + 2e^{-} \rightarrow 2OH^{-}$$

This current flow is then converted by Faraday's law to metal loss :

$$m = M\ I_c t/zF$$

Where m is the mass of steel consumed, Ic is the current in amperes, t is the time in second, z is the ionic charge(2 for $Fe \rightarrow Fe^{2+} + 2e^-$), F is the Faraday constant and M is the atomic weight of the metal.

2.7.1.1 Corrosion Potential and Potential Mapping Measurements

This consists of the determination of the voltage difference between the embedded steel and a reference electrode in contact with the grout. A good contact between the reference electrode and the grout must be ensured in order to minimize the ohmic drop. ASTM standard C -876 - 91 describes the method and indicates the potential ranges in relation to the probability of corrosion in chloride contaminated concrete as shown in table 2.1. Though potentials do not provide information on the amount of corrosion, the measurements of the potential gradients created by the corrosion process allows areas of possible corrosion to be identified. It must however be noted that factors such as material inhomogeneity, moisture content, etc, could lead to misleading potential values (14).

Table 2.1: ASTM C-879-91 Corrosion Potentials Interpretations

PROBABILITY OF CORROSION	CORROSION POTENTIAL(Cu/CuSO4)
> 95 %	< - 350mV
< 5 %	> - 200 mV
Approximately 50%	-200mV to -350 mV

2.7.1.2 Resistivity Measurements

The electrical resistivity of concrete or mortar is an indication of the amount of moisture in the pores, and the size and tortuosity of the pore system. It is strongly affected by the permeability of the material, which is dependent on curing, additives used and water to cementitious materials ratio.

Chloride levels do not seem to affect resistivity directly as the ions already in the pore far exceed any chloride ions which might infiltrate into the system. The hygroscopic nature of chlorides might however encourage the grouts to retain water and subsequently reduce the resistivity. Broomfield et al (18), using field polarization device for corrosion measurements found the following correlation between resistivity and corrosion rates for concrete rebars.

> 100 kΩcm Cannot distinguish between active and passive steel.

50 - 100 kΩcm Low corrosion rate.

10 - 50 kΩcm Moderate to high corrosion where steel is active.

< 10 kΩcm Resistivity is not the controlling parameter.

2.7.1.3 Polarization Resistance Measurements

The linear polarization resistance technique involves the polarization of the steel with an electric current and the subsequent monitoring of the effect on the half cell potential.

By the use of a low voltage power supply and an auxiliary electrode, a small current is passed from the auxiliary electrode to the embedded steel (Working electrode).

Stern et al. (15) showed that for a simple model corroding system, the polarization curve for a few millivolts around the corrosion potential approximately follows a linear relationship. The slope of this relationship was referred to as the Polarization resistance (R_p).

The electrochemical measurement carried out is basically a determination of the polarization resistance (R_p). For the region a few millivolts around the corrosion potential, the slope is given by $R_p = (\Delta E/\Delta I)_{\Delta E \to 0}$. This slope is related to the instantaneous corrosion rate through the Stern - Geary Equation (15).

$$Icorr = \frac{B}{R_p} \qquad \text{Where } B = \frac{\beta_a \times \beta_c}{2.3 \times (\beta_a + \beta_c)}$$

β_a and β_a are the Tafel slopes for the anode and cathode reactions respectively. The value of B have been determined to lie between the range of 26 and 52mV for rebars in concrete (depending on the passivity or active condition of the steel) (15) .

A plot of change in current versus change in potential gives a gradient of the polarization resistance from which the corrosion rate can be calculated from the equation;

$$CR = 11 \times 10^6 \, B/(Rp \times A)$$

Where Rp = The polarization Resistance.

A = The surface area of steel measured in centimeters.

CR = Corrosion Rate in μmy^{-1}.

B = Constant (26 to 52mV for steel in concrete).

The measurement is accomplished in two ways, either steady fixed currents are applied and the potential monitored (galvanostatic) or the current is measured to achieve one or more predetermined potentials (Potentiostatic). In both cases, allowance for the ohmic drop are made. Periodic measurements are performed and corrosion rate values are plotted as a function of time. The limitation of the linear polarization method is the uncertainty in the determination of the steel area measured.

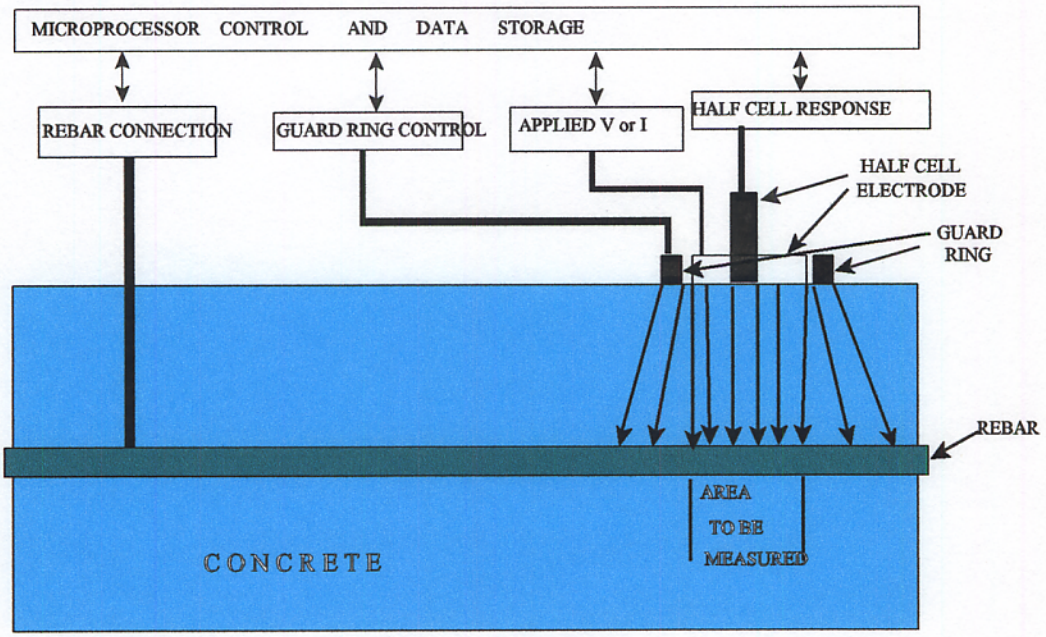

FIGURE 2.6 : Schematic of Linear Polarization Device with Censor Controlled Guard Ring for Defining Area Measured (J.P. Broomfield : Corrosion of Steel in Concrete)

Some manufacturers have developed a guard ring system to confine the area of the current. Figure 2.6 illustrates the guard ring concept for linear polarization measurement.

2.7.1.4 Electrochemical Impedance Spectroscopy (EIS) Measurement

Feliu et al (16) used this technique, which consists of the application to the working electrode of a small amplitude (a few millivolts, ΔE , peak to peak) sinusoidal voltage over a wide frequency range by means of a digital frequency analyzer (or Transfer Function Analyzer). The current response at every frequency is another sinusoidal signal with a different amplitude (measured as ΔI) and a phase shift relative to the input signal. The ratio $\Delta E/\Delta I = Z$, is the impedance of the system which is frequency dependent.

The A.C Impedance technique has been found to be less accurate than the Polarization Resistance technique because of the uncertainty in graphical extrapolation and mathematical calculation involved. The impedance technique is also more time consuming and requires expensive equipment and some computational power to elaborate the result. The linear polarization resistance technique is therefore preferred for use for both the laboratory and field corrosion measurements.

2.7.2 Non - Electrochemical Techniques

The two non-electrochemical methods commonly used to assess the corrosion of metals are visual assessment and weight loss measurement.

2.7.2.1 Visual and Microscopic Observations

Visual and microscopic observations of the corroded surface may provide approximate information about the depth of the attack, the number of pits or the proportion of the attack area. This method is mainly used to confirm the findings of other methods.

2.7.2.2 Weight Loss Technique

This technique consists of weighing the specimens before and after being introduced into the grout to be tested. The method for corrosion evaluation using the weight loss of a corroded metal has been described in ASTM - G1 -1991 (19). For iron and steel, hot sodium hydride was recommended for cleaning the rust, however, this involves some hazards and more sophisticated equipment.

The use of Clarke's solution, consisting of the following was therefore recommended;

Hydrochloric Acid (Specific gravity = 1.19)	=	1liter
Antimony Trioxide (Sb_2O_3)	=	20g
Stannous Chloride($SnCl_2$)	=	50g

Cleaning should be at room temperature for a time period up to 25 minutes.

A brass bristle brush or brass scraper or both can be used in place of chemical cleaning, followed with a wet bristle brush and fine scouring powder.

CHAPTER 3
DEVELOPMENT OF EXPERIMENTAL PROGRAMS

3.1 Objective of Experimental Program

The objectives of the experimental programs are :

1) To investigate the corrosion of embedded bolts and nuts in the grouted base plate assembly and compare this with that of the assembly without grout and determine if the use of grout pad under the base plates in the signing and lighting poles has any advantage.

2) To investigate the adequacy of the cover of the grouted base plate arrangements in practice.

3) To compare the effect that water absorption of the grouts has on the corrosion of the bolts and nuts of the base plate arrangements.

3.2 The Experimental Design

For a given temperature, the main variables that will affect the corrosion of embedded steel in the grouted base plate arrangement are the ease of transport of aggressive ions through the grout cover, the length of time that the grout will retain moisture after getting wet (which affects the resistance of the grout to flow of electrons) and the presence of aggressive materials in the grout formulation.

Three grouts which had been approved by the Florida Department of Transportation (FDOT) were selected for the experiment based on their compressive strength and setting times . Two test samples (Based on Halls(13)) were prepared from each of the three selected grouts and absorption tests performed on them to select the two grouts with the highest and lowest absorption rates. Tests for compressive strength and unit weights of the grouts were conducted to correlate the results with the absorption test results.

Each of the two selected grout types were used for the construction of two replicates of the grouted base plate arrangement for signing and lighting posts in accordance with FDOT specifications. Two other specimens were constructed without the use of any grout between the base plate and the concrete base. The three grouts selected for the absorption tests were labeled Grout Type A, Grout Type B and Grout Type C .

Two circular plastic tanks, each measuring 6 feet (1.83 meters) in diameter and 2.0 feet (0.60 meters) in depth were used to hold the samples for the accelerated corrosion tests. Each tank was used to hold one sample with the grout of high absorption(Grout Type A), one sample with the grout of low absorption (Grout Type B) and a third sample without a grout pad. One tank was filled with sodium chloride solution of 3.5% concentration to a level midpoint of the galvanized steel baseplate. The sodium chloride solution was alternatively pumped from one tank to the other by the use of a submersible pump in accordance with the schedule shown in Table 3.1.

Table 3.1 : Program for Wet-Dry Cycling and Electrochemical Measurements

Period (days)	Cycling In Tank 1	Cycling In Tank 2	Remarks
1 - 14 days	24 hrs wet-24 hrs dry for both tanks		
15 - 28 days	24 hrs wet-24 hrs dry for both tanks		Measurement at begining of the 15th day for 24 hours (Both tanks)
29 - 35 days	Wet for first 84 hours (31/2 days) and 24 hrs wet-24 hrs dry for remaining days.	Dry for first 84 hours (31/2 days) and and 24 hrs wet-24 hrs dry for remaining days.	Measurement at begining of 29th day for 84 hours (tank 2)
36 - 42 days	24 hrs wet-24 hrs dry for both tanks		
43 - 56 days	24 hrs wet-24 hrs dry for both tanks		Measurement with RPX1 at the end of 6 weeks
57 - 67 days	Wet throughout	Dry throughout	Measurement for 10 days (tank 2), both instruments
68 - 74 days	Wet for first 3 days, followed with drying for 1 hour and wet for remaining 4 days.	Dry for first 3 days, followed with wetting for 1 hour and dry for remaining 4 days.	Measurements in tank 2 for 4 days at end of 10th week
75 - 78 days	Dry for first 30 minutes, followed with wetting for 3 days.	Wet for first 30 minutes, followed with drying for 3 days and	Measurements in tank 2 for 3 days.
78 - 91 days.	24 hrs wet-24 hrs dry for both tanks		
9 2- 98 days.	Wet for first 5 days	Dry for first 5 days	Measurement (tank 2) after 13 weeks

Electrochemical measurements were taken to evaluate the rate of corrosion of the bolts and nuts in the base plate assemblies for various time periods were taken with the P-R monitor and RPX1 corrosion transmitter.

The duration of measurements were varied to obtain an understanding of the corrosion behavior after long periods of drying of the samples

The concentration of the salt solution was periodically checked with a hydrometer and any increase in concentration due to the evaporation of water from the tanks were corrected by the addition of more water to keep the concentration constant. The grouts were cut open at the end of fourteen weeks and visual inspection made on the embedded steel.

3.3 Fabrication of Test Specimen

3.3.1 Materials

3.3.1.1 Concrete

The concrete used for the foundation of the base plate arrangements was a ready - mix concrete designed to meet DOT specifications for class II concrete. The minimum design compressive strength was 23.45 Mpa (3400psi) at 28 days.

3.3.1.2 Base Plates

The base plate material was an ASTM A 36 clean mill steel galvanized per ASTM A 123 and in accordance with FDOT specifications.

3.3.1.3 Anchor Bolts, Nuts and Washers

The anchor bolts, nuts and washers were fabricated in a local shop with steel meeting the ASTM specifications shown in table 3.2.

Table 3.2: Specifications for Anchor Bolts, Nuts and Washers.

Part Description	ASTM Specification
Anchor Bolts	ASTM F1554 Grade 380
Washers for Anchor Bolts	ASTM F436M Type 1
Nuts For Anchor Bolts	ASTM A563M Class 8S or 8S3

The specifications were in accordance with FDOT specification requirements for cantilever arm mounted traffic signal structures.

3.3.1.4 Grouts

Three manufactured non - shrink grout types A, B and C which had been pre-approved by the FDOT for use in the construction of the base plate arrangement were used. Table 3.2 shows the properties of the three selected grouts obtained from the manufacturers.

Table 3.3: Manufacturers' Specifications for Selected Grouts

Grout Type	Compressive Strength		Initial Setting Time	Mixing Water/bag	Flow at Mixing
	7 days	28 days			
A	8,000psi	-	4.0 hours	1.26 gals	30 secs
B	6500psi	7500 psi	4.0 hours	About 1.26 gals	25 to 30 secs.
C	Not Available			9.5 pints	Meeting ASTM C939

3.3.2 Dimensions

The typical dimensions of the anchor bolts, base plates and foundation concrete used in the experimental program are presented here.

3.3.2.1 Anchor Bolts

The anchor bolts were 19.0 mm (3/4") diameter cold rolled structural steel rods that were threaded on each end. They were 330.2 mm (13.0") long with 88.9 mm (3.5") of thread on the embedded end and 127.0 mm (5 inches) of thread on the exposed end. Figure 3.1 shows a typical drawing of an anchor bolt. The length of thread was determined from typical shop drawings of base plate connections by the FDOT. However, the thread on the embedded end was shortened since the bolts would not perform any structural function during the testing.

3.3.2.2 Base Plates

The base plates were annular (i.e circular with a circular hole in the middle). The dimensions, which were in accordance with FDOT specifications are shown in a typical plate shop drawing in Figure 3.2. The plate is an 18 inches (457.2 mm) in diameter, 1 inch (25.4 mm) thick with a 12 inches (323.85 mm) hole in the middle. Eight anchor bolt holes were drilled on a radius of 15 inches (381.0mm) on the plates at equal spacings.

.

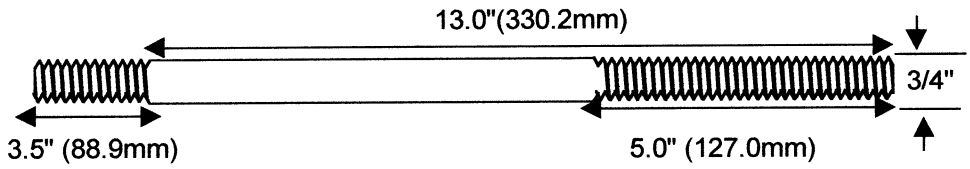

Figure 3.1 Typical Drawing of Anchor Bolt.

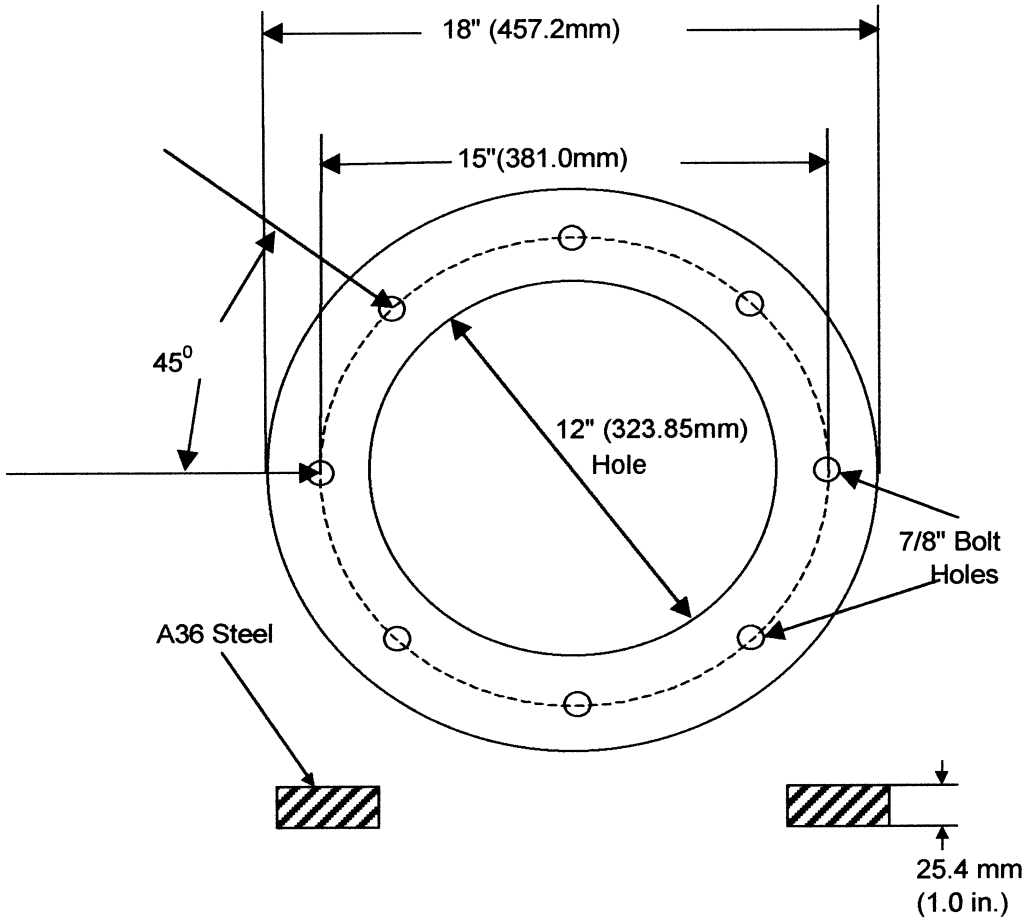

Figure 3.2 Typical Drawing of Base Plate.

3.3.2.3 Concrete Foundation

A typical foundation for the corrosion test was 24 inches (609.6 mm) x 24 inches (609.6 mm) x 9 inches (228.6 mm) thick unreinforced concrete foundation block with the anchor bolts inserted at the time of casting on a 15 inch diameter circle at the top of the foundation block. The 5 inches length of the anchor bolt was left to protrude at the top of the foundation block. (Figure 3.3).

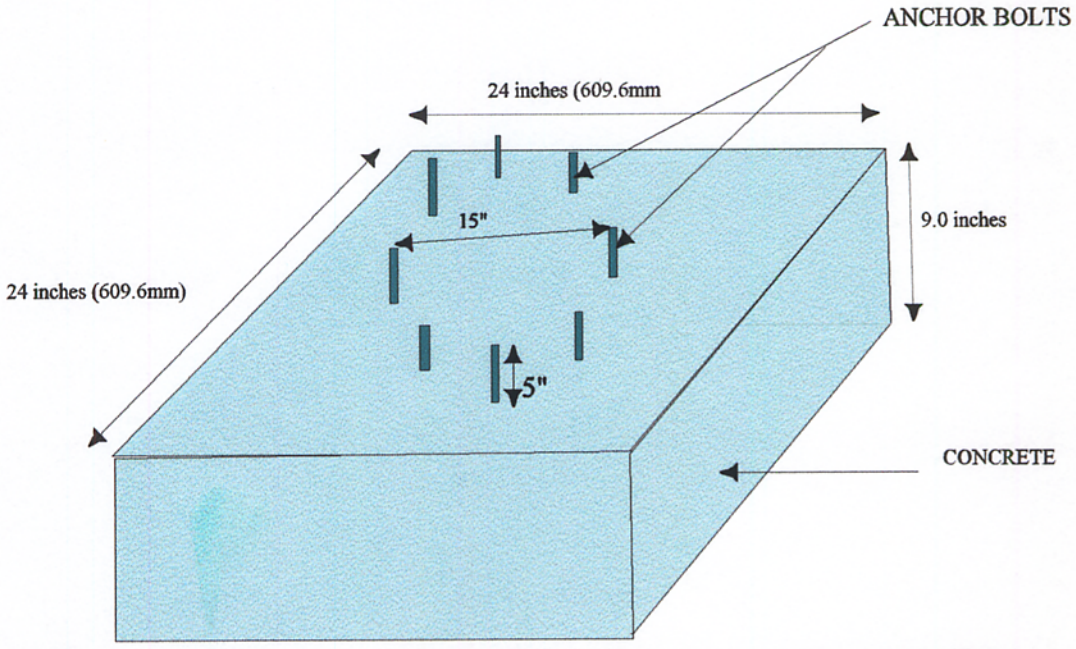

Figure 3.3 Foundation of Base Plate Arrangement with inserted Bolts.

3.3.3 Fabrication of Concrete Base

The concrete bases were cast using ready - mix concrete. The concrete was consolidated during placement with a hand - held mechanical vibrator. After filling the forms, the surfaces were screeded, troweled and covered with a polyethylene sheet to aid curing. The formwork was constructed from 3/4 inch thick plywood and had 24 inches (600 mm) x 24 inches (600 mm) x 9 inches (230 mm) internal dimensions. The formwork was fabricated to stand on the side (9 inch side as base) for ease of inserting the anchor bolts.

All anchor bolts were cast-in-place and were installed with 3/4" plywood templates with 7/8" holes at the anchor bolt positions attached to the formwork by 3" nails to hold the bolts in the proper position at the correct embedded length during concrete placement. The bolts were attached to the template with nuts on each face of the template. The embedded end of the bolt was 1.0" (25.4 mm) from the base form and was single nutted.

The formwork was lubricated with SAE-30 motor oil prior to pouring of the concrete to facilitate its removal. They were stripped within seven days after casting. Further work on the blocks was suspended for 28 days.

3.3.4 Mixing of Grouts

Mixing of the gout was accomplished by the use of a drilling machine to which is attached a mixing paddle with four blades. The inside of a plastic bucket was first dampened, the required amount of water was measured with a graduated cylinder and poured into the bucket, the mixing paddle was turned on and the required quantity of grout was gradually poured into the water while the paddle is still on and slowly churning

the water. The operation of pouring the grout was accomplished within two minutes. After completely adding the grout, mixing was continued for 3 to 3-1/4 minutes at a high speed. Immediately on completion of mixing, the flow for each grout mix was determined in accordance with ASTM C939-94a - Standard Test Method for Flow of Grouts for Preplaced - Aggregate Concrete (Flow Cone Method). 4"(100 mm) x 8" (200 mm) cylinders were poured for each grout for the absorption test specimen. The grouts were also poured into 2"(50 mm) x 2" (50 mm) molds for the compressive strength tests and the determination of unit weights of the grouts.

3.3.5 Grouting of Base Plate Arrangement

The base plate was fixed onto the foundation base by first screwing a hexagonal nut on each anchor bolt to act as adjusting screws for the plate. This was followed by the mounting of the plates, adjusting the bottom screws to insure that the plate is level and finally tightening it up at the top with double nuts.

A circular metal formwork, 18.0" (457.2 mm) in diameter and 2" deep was placed around the plate and made to hold the fluid grout between the plate and the top of the base concrete by sealing all spaces with a caulk. The metal formwork was held in position by screwing it onto the concrete base.

The grout was poured into the steel formwork, making sure that it was completely filled and the grout was in contact with the bottom of the base plate. The grout was then gently tamped with a 3/4" rod to insure that it flowed into all corners. The metal formwork was removed after seven (7) days and the test specimen were left for at least 28 days before any further work was done on it.

Each of the two grouts selected as a result of the water absorption test was used on two base plate arrangements to produce two replicate samples for the corrosion testing. Two of the base plate arrangements were used as control and therefore had no grout pads. The pictures in Figures 3.4, 3.5 and 3.6 show the completed base plate arrangement test specimen for the corrosion testing.

3.4 Tests on Hardened Grout

The cube compressive strength and water absorption tests were carried out on the hardened grouts. The unit weights of the three grouts were also determined.

3.4.1 Compressive Strength Test

Compressive strength tests were performed in accordance with ASTM C - 942, test for compressive strengths of grouts for preplaced - aggregate concrete in the laboratory (23) on cubic specimens measuring 2"(50 mm) x 2"(50 mm) x 2"(50 mm) . The compressive strengths were determined for ages 7 and 28 days after curing in the moist room in accordance with ASTM test method C109.

The compressive strength was calculated as follows;

$$f'_c = P/A \quad \text{----------} \quad 3.1$$

Where

f'_c = Compressive strength, Psi.

P = Maximum load carried by specimen (lbs) and

A = Average cross sectional area of the specimen.

Figure 3.4: Base Plate Assembly Test Sample With Grout Pad

Figure 3.5: Base Plate Assembly Without Grout Pad

3.4.2 Determination of Unit Weight

The unit weight of the grouts were determined in accordance with ASTM C938 section 9.6.1. Measurements of each dimension of the 2"(50 mm) x 2"(50 mm) x 2"(50mm) cubes were taken twice to the nearest 0.25mm and the volume computed based on the average measurements. The weight of the specimen is then divided by the measured volume to obtain the unit weight.

3.4.3 The Water Absorption Test

A simple laboratory method similar to the one described by Hall(13) was used to determine the rate of water absorption of the grouts. The surface water absorption, or sorptivity can be determined by measurement of the capillary rise absorption rate on the grout test specimen. The specimens were 4 inches (101.6 mm) in diameter by 5 inches (127mm) in height cut from the 4" (101.6 mm) by 8" (203.2 mm) laboratory cylinder specimen.

The specimen were oven dried at 105^{o}C (221^{o}F) for 24 hours, and were allowed to cool for 1 - 1-1/2 hours after removing from the oven. The lower part of the sides of the specimen adjoining the inflow face were sealed with adhesive tape. The specimen were made to rest on rods to allow free access of water to the bottom (inflow face). The water level was not more than 1/4" or so above the base of the specimen. Figures 3.6 and 3.7 show pictures of the absorption test specimen and the absorption test set up respectively.

The quantity of absorbed water is measured at intervals by weighing the specimen on a top pan balance weighing to 0.1 gram. Surface water on the specimen was mopped

off with a dampened rag before weighing. Each weighing operation was completed as quickly as possible (within 30 seconds). Measurements in this experiment were taken at 10, 20, 30, 45 and 60 minutes after starting the test. The dimensions of the specimens and the temperatures were also taken.

Theoretically, the cumulative water absorption (per unit area of inflow surface), 'i', increases as the square root of time (see section 2.4.2) . The relation can be shown as equation 3.2.

$$i = St^{1/2} \quad \text{---------- 3.2}$$

Where

$i = \Delta w/A\rho$, i.e volume of water flowing through unit area of grout ml/m^2.

Δw = The increase in weight in grams.

A = Area of the inflow surface, m^2.

ρ = Density of water g/cm^3

t = Elapsed time in minutes.

S = The sorptivity, which is the slope of the 'i' versus $t^{1/2}$ plot in $ml/m^2/min^{1/2}$.

Figure 3.6: Water Absorption Rate Test Specimen

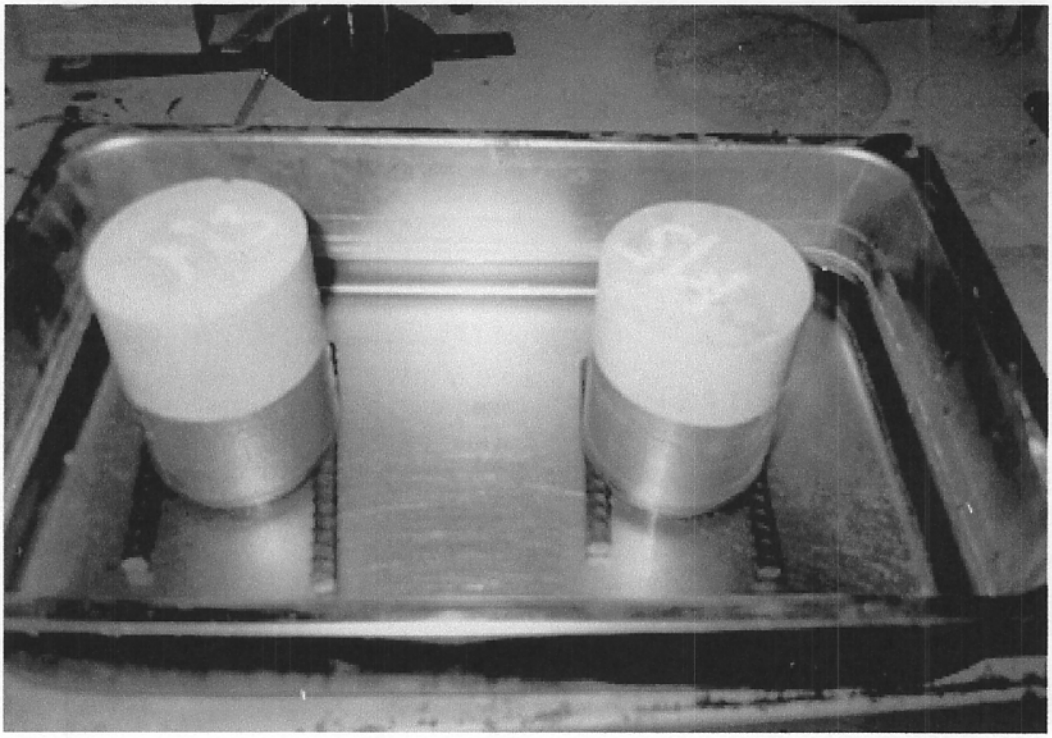

Figure 3.7: Water Absorption Rate Test Setup

3.5 Corrosion Testing

At 28 days after pouring the grout pads for the base plate arrangements, three base plate test specimens, one without a grout pad and the other two with grout pads made of the selected grouts were mounted in each of two plastic tanks as described under section 3.2. The tanks were filled with salt water of 3.5% concentration and kept in a laboratory room where the temperature was maintained between 74 to 76^{O}F. The salt water was recycled between the two tanks and corrosion measurements were taken in accordance with the program shown in Table 3.1. Figure 3.8 shows the corrosion test set up.

3.5.1. Equipment

The P-R Monitor version 4.40C manufactured by Cortest Columbus Technologies, Inc was used in monitoring the corrosion activities in the system. The equipment consists mainly of a potentiostat with electrode connectors to which is attached a PC notebook containing programs which permit the selection of voltage step size, number of steps, time between each step, and potential with respect to the free corrosion potential for beginning the stepping sequence.

The equipment measures an apparent polarization resistance PR$^{/}$ (PR$^{/}$ =PR +Rs) using the standard D.C technique, followed by the measurement of Rs by the AC technique. PR is then calculated as PR$^{/}$ - Rs. At the end of the standard polarization measurement cycle, an AC signal is automatically applied to the working electrode for the purpose of measuring the solution resistance (Rs). The equipment is powered by a 120 V AC but had an optional internal battery supply.

The P-R Monitor is capable of ± 10volt output between the counter and working electrode leads and can supply up to 50 mA of current.

The P-R monitor is equipped with a guard ring counter electrode which consists of a central counter electrode (CE) and a separate "guard ring" electrode which surrounds both the central electrode and reference electrode. The purpose of the guard ring is to better confine the counter electrode current to the area directly below the central electrode, and thus allow a more accurate calculation of the corrosion rate. Figure 3.9 shows a picture of the P-R monitor version 4.40C and Figures 3.10 and 3.11show a diagram of the assembly configuration of the guard ring electrode and the electrode setup in the experiment respectively. The electrode cables connect to the instrument via a 6-PIN connector located on the left side of the instrument. Connection to the auxiliary electrode is made with a 5-PIN AMPHENOL connector (MIL -C -5051), located on the top of the electrode. The reference electrode is connected using a white clip attached to the electrode cable. A black clip cable lead is provided for connection to the working electrode.

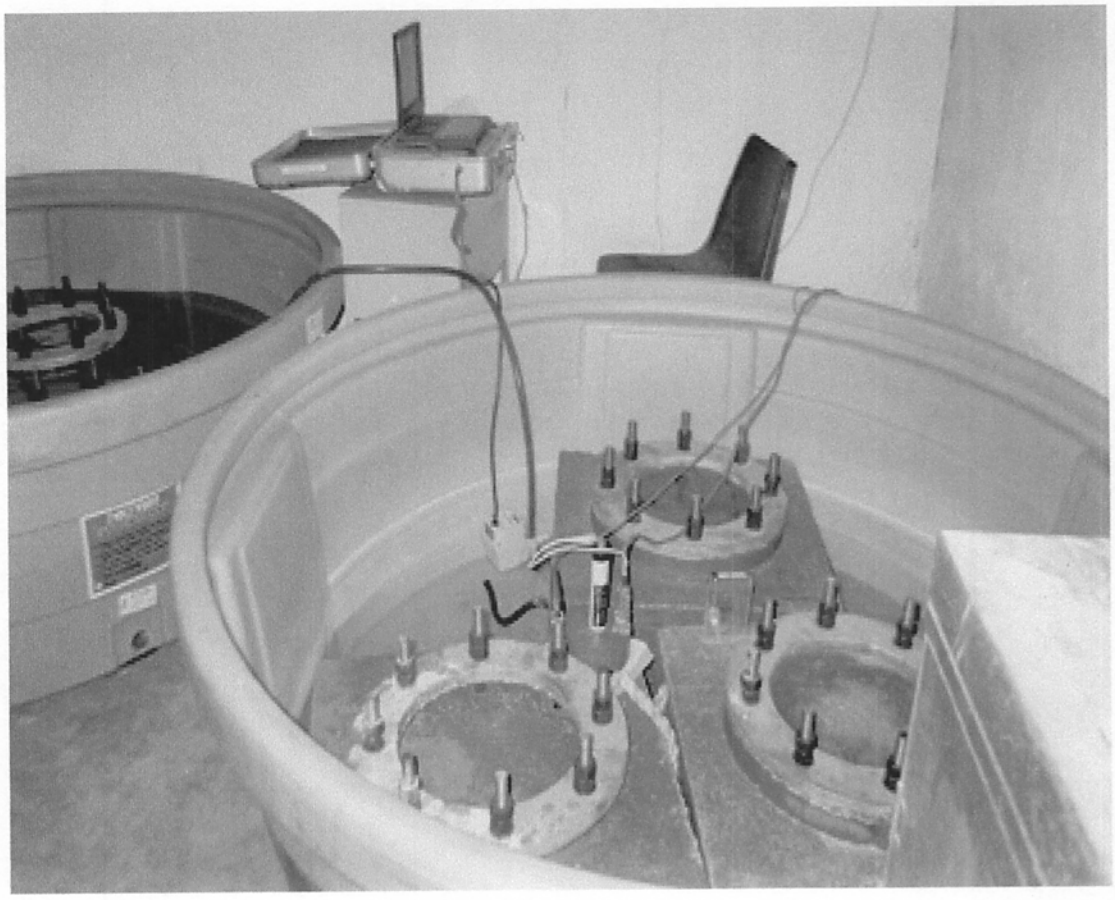

Figure 3.8: Corrosion Rate Test Setup

Figure 3.9: P-R Monitor Version 4.40C

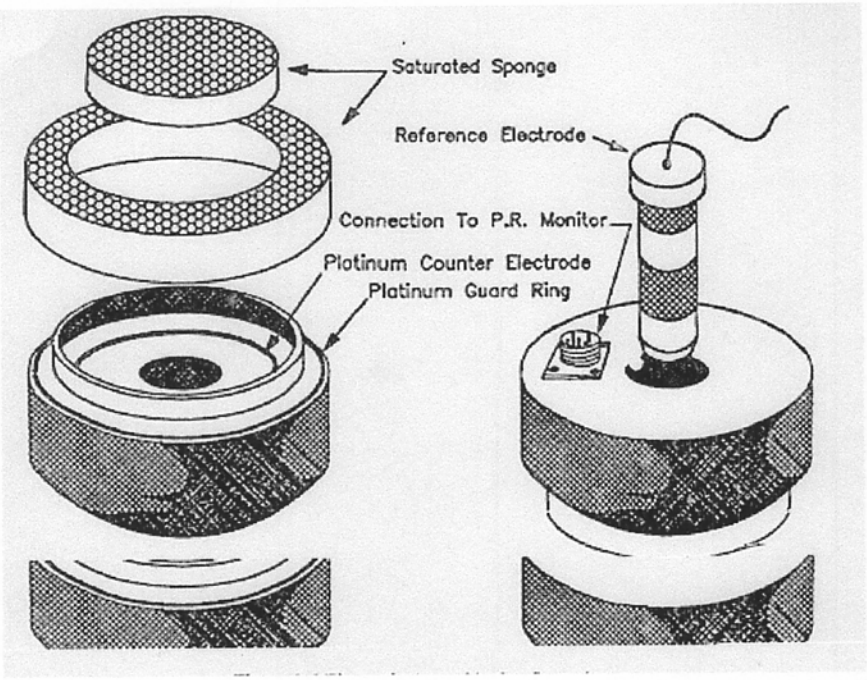

Figure 3.10: Electrode Assembly Configuration

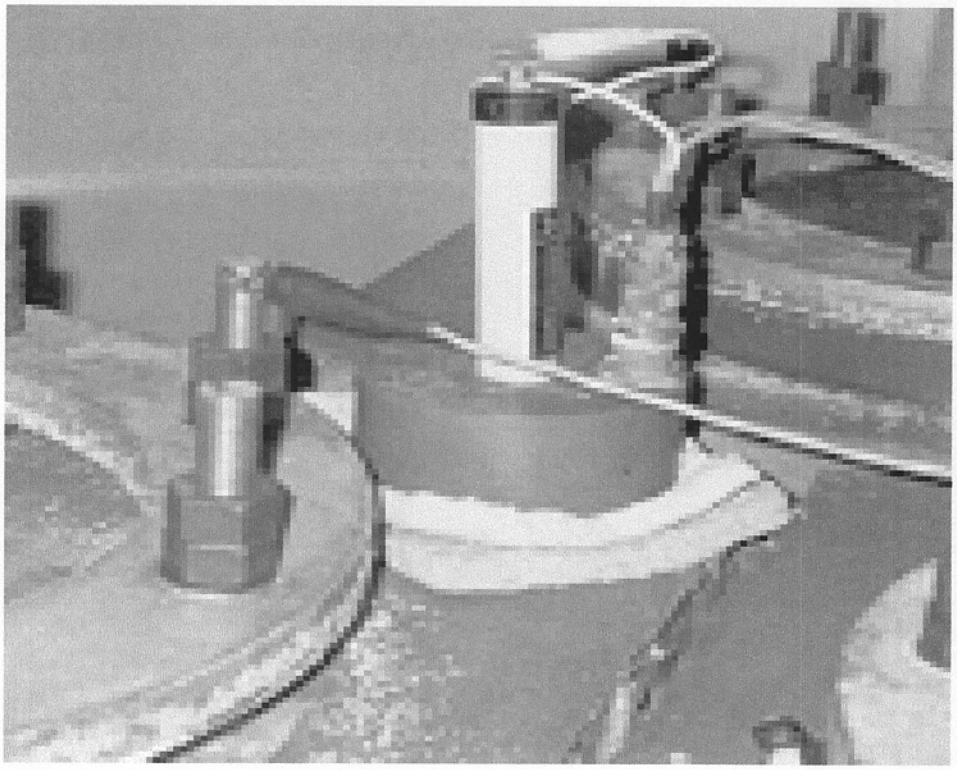

Figure 3.11: Guard Ring Electrode Connection to an Anchor Bolt

3.5.1.1 Theory of P-R Monitor Corrosion Measurements

The Corrosion rate (CR) is calculated by the following formula, which is derived from Faraday's law;

$$CR = I_c \times M \times X / F \times z \times D \quad \text{----------3.3}$$

Where CR = Corrosion Rate

Ic = Corrosion Current

M = Atomic Weight of the Electroactive species (56g for iron).

F = Faraday's Constant, 96,487C/g-equivalent.

X = A conversion Factor for units

z = The ionic charge (2 for $Fe \rightarrow Fe^{2+} + 2e^{-}$).

D = Represents the diameter of guard ring electrode.

A material constant, MC = M x X / F x z x D was defined for the instrument and this was taken as being equal to 11619 for iron.

Also from the Stern - Geary equation, Ic = B/Rp - - - - - - - - - - - - - - - - - - -3.2

B in this equation was denoted as EC, which is the Environmental constant. The value of the environmental constant is set at 0.035V, which corresponds to $\beta a = 0.16V$ and βc of 0.16V in the Stern - Geary relationship. These values are typical of reinforcing steel in concrete.

3.5.1.2 Operation of the P -R Monitor

The P - R Monitor 4.40C uses an analog potential control stepping sequence. The software allows for the programming of the following:

(1) Minutes between tests

(2) Number of steps for each step

(3) Seconds between each step

(4) Voltage drop between steps

(5) Potential over corrosion potential to start

(6) Unit preference (English or Metric) , and

(7) The rebar number (This allows the equipment to determine the rebar diameter)

By providing these input parameters, the average scan rate for the polarization resistance test can be controlled and the test duration could subsequently be fixed. The output from the P-R monitor is a plot of the applied voltages versus the corresponding currents in the vicinity of the corrosion potential to determine the polarization potential ($PR^{/}$).

At the end of the standard polarization cycle, an AC signal is applied to the working electrode for the purpose of measuring the solution resistance Rs, after which the previously determined $PR^{/}$ is corrected to $PR = PR^{/} - Rs$. The software thereafter outputs (1) The instantaneous corrosion rate in either mpy (mils per year) or μmy^{-1}(micrometer per year), (2) the corrosion potential in mV, (3) the solution resistance in ohms and (4) the polarization resistance in ohms.

3.5.1.3. Linear Polarization Measurements

The linear polarization technique was used in the corrosion testing with the P-R Monitor 4.40C as follows;

(A) The guard ring electrode of the monitor was placed on the base concrete foundation at a corner nearest to the anchor bolt for which corrosion was to be

monitored. The cable for the working electrode was connected to the top of the anchor bolt. Figure 3.11 shows a diagram of the connection of the P-R Monitor (Only one bolt is shown for clarity) . It was estimated that with this arrangement, the guard ring would direct the electrical signal onto a specified area on the anchor bolt where anodic dissolution was taking place in the form of corrosion as indicated by arrows showing the flow of the electrical signal to the anchor bolt in Figure 3.12.

Figure 3.13 shows a plan view of a test specimen with indications of guard ring electrode positions and corresponding anchor bolts for which corrosion is monitored.

The P-R Monitor was set to the following configuration;

(1) Number of tests run 1

(2) Minutes between each test 10

(3) Number of steps for each test 7

(4) Seconds between each step 15

(5) Voltage Drop Between each Step 5 mV

(6) Potential over Corrosion Potential to Start 15 mV

(7) Pretest Potential Drift ? Yes

(8) Unit Preference English , and

(9) Rebar Number 6 (For 3/4 diameter steel).

(C) Measurements were made on four anchor bolts per base plate arrangement, amounting to 12 measurements for the three base plates. Successive measurements were however made on anchor bolts at similar locations on the base plate from test specimen 1 (With no grout pad) followed by specimen 2 (With grout type A) and then specimen 3 (With grout type B).

This sequence was followed till all 12 anchor bolts are measured. One complete measurement took about 2 hours

3.5.1.4 The RPX1 Corrosion Transmitter

A second instrument, the RPX1 corrosion transmitter, which also measures corrosion potentials and currents was used . This instrument is also based on the polarization resistance measurements described above, however with the use of a reference electrode directly placed on the surface of the grout pad nearest to the bolt for which corrosion is monitored. In the case of the assembly without grout, the reference electrode was paced directly in contact with the exposed anchor bolt between the base plate and foundation concrete. The main difference between the RPX1 and the PR-Monitor is in the electrode configurations. The RPX1 is not equipped with a guard ring electrode.

3.5.2 Visual Assessment

At the end of 14 weeks of wet - dry cycling, the base plates were dismantled and the grout pads of the grouted base plate specimens were cut open to reveal the anchor bolts. Visual observations were made and photographs of the three specimens showing the exposed bolts were taken. Photographs of the dismantled base plates were also taken with a digital camera at close range.

3.5.3 Weight Loss Measurements

After the visual observations, the bolts on each of the six base plate assemblies were unscrewed. Care was taken to ensure that rust materials which were removed during the unscrewing of the bolts were collected on a piece of paper. The weight of the rusted bolts were then taken together with any rust removed during the unscrewing of the bolts.

The rusts were then removed from the bolts with a brittle wire brush in accordance with ASTM test specification G1 - 1991 as described under section 2.6.2. of this report.

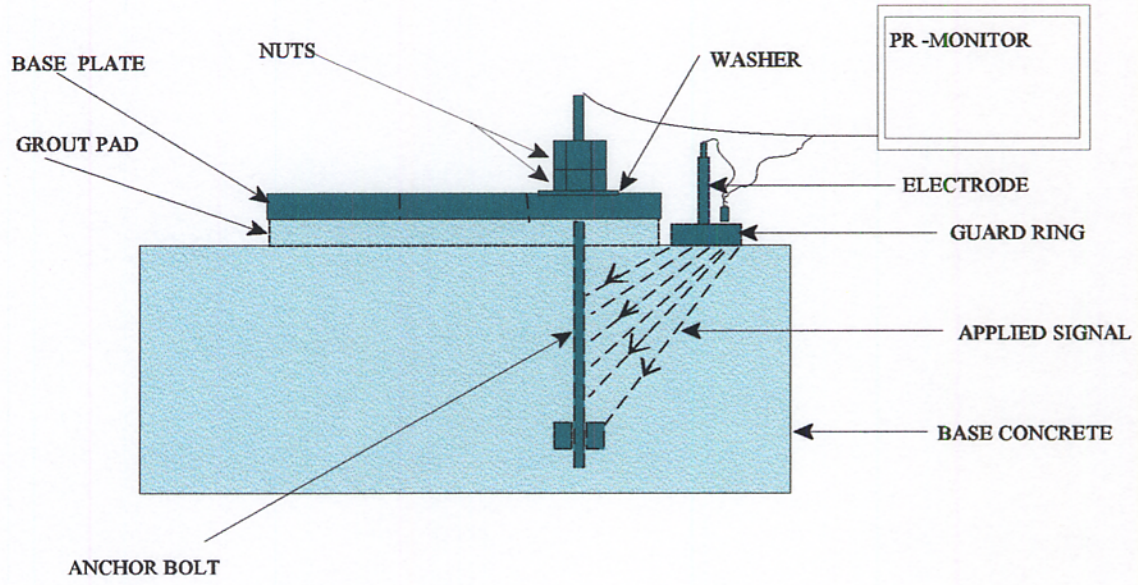

FIGURE 3.12: INSTALLATION OF PR MONITOR SHOWING MEASUREMENT ON A SINGLE ANCHOR BOLT

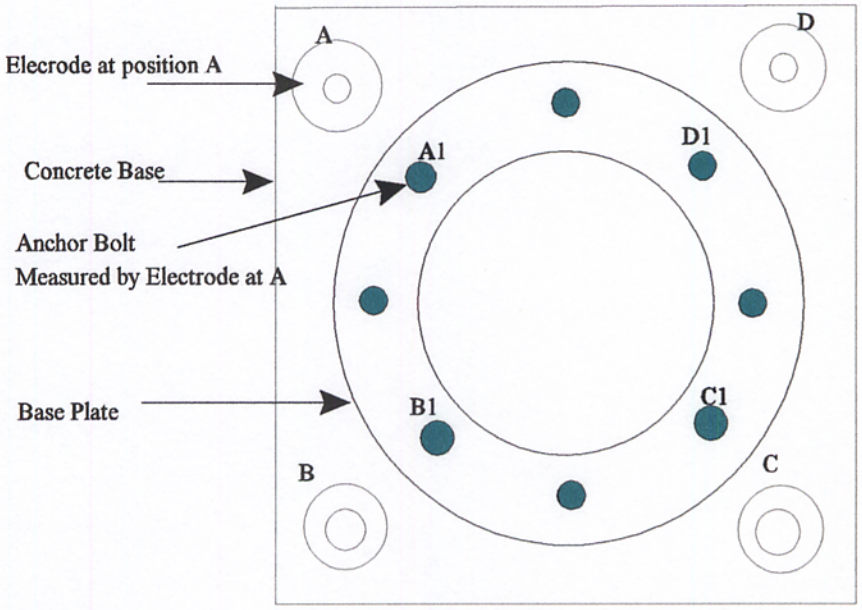

FIGURE 3.13:POSITIONS OF GUARD RING ELECTRODE AND RESPECTIVE POSITIONS OF ANCHOR BOLTS MONITORED (A1, B1, C1 AND D1)

CHAPTER 4
RESULTS OF TESTS ON HARDENED GROUTS

This chapter presents the results of unit weight, compressive strength and water sorptivity tests conducted on the three grouts prior to the selection of two for the corrosion testing. Details of the experimental designs, methods of analysis and laboratory procedures used have been explained in chapter 3.

4.1 Unit Weight of Grouts

The results of unit weight calculations for the grouts as well as quantity of water and grout used for mixing are displayed in table 4.1. These results are fully discussed in section 4.4. Unit weight measurements were done on three replicates per grout. The three replicates were obtained from the same mixes used to perform the water absorption tests. Appendix A shows the results of the individual tests.

Table 4.1: Flow, Unit Weights and Mixing Quantities for Grouts.

Grout Type	Wt. of Grout (kg)	Vol. of Water(l)	Flow (Flow Cone)	Mean Unit Wt (pcf)	Standard Deviation of Unit Wt (pcf)
A	8,000	1,600	30 secs	127.32	2.45
B	8,000	1,640	26 secs	135.83	2.19
C	8,000	1,500	26 secs	135.75	1.36

4.2 Results of Compressive Strength Test

The results of the compressive strength tests performed on the three grouts are shown in table 4.2 . The compressive strengths obtained from the laboratory were compared with the manufacturer's stated strengths (94.3% for the 7 day strength for grout type A, 116% and 112.3% for the 7 day and 28 day compressive strengths for grout type B respectively). The compressive strengths for grout type C was the highest. The results of the compressive strength tests are further discussed under section 4.4. The compressive strength tests were done on three replicates per grout at both 7 days and 28 days moist curing.

The three replicates were obtained from the same mix used to perform the water absorption tests. Appendix A shows the individual test results.

Table 4.2: Results of Compressive Strength tests on Grouts.

Grout Type	Mean Compressive Strength (psi)		Standard Deviation (psi)	
	7 Days	28 Days	7 Days	28 Days
A	7,543 (94.3%)	8,198 (-)	642	9.0
B	7,548 (116 %)	8,420 (112.3 %)	359	241
C	7,957 (-)	9,223 (-)	83	229

Manufacturer's specified strengths for grout type A for 28 days and grout type C for both 7 and 28 days were not available.

Values given in brackets represents the percent of the manufacturer's stated grout strengths.

4.3 Absorption Test Results

The water absorption test described in chapter 3 was performed on the hardened grouts after 28 days of moist curing. Two replicate specimens were tested for each of the three selected grouts. A cross sectional area of 81.07 cm^2 was used in the sorptivity calculations. The water temperature was in the range of 76 to 82^{O}F during the experiment. Therefore a density of 997g/cc for water was used in the sorptivity calculations. Room temperature at the time of testing was 84^{O}F. The water sorptivity of the grouts in this study were determined using equation 2.2.

The test results are summarized in table 4.3, Figure 4.1 shows the sorptivity plots, or plots of "i" (volume of water per unit area of grout) against the square root of time in minutes ($t^{1/2}$) of the 28 days moist cured specimens for grout types A, B and C. (The average results of two tests per grout type were plotted). The results of calculations are shown in Appendix B.

4.4 Discussion of Results of Tests on Hardened Grouts

Comparison of the effect of the quantity of mixing water requirements of the three grouts on compressive strength could not be made in this project because the composition of the grouts were not made available. It is believed that the three grouts have different cementitious material composition and different types of admixtures to make them stable at the fluid consistency at which the grouts were mixed. The different quantities of water used in mixing could be a source of comparison based on the water/ cement ratio which determines to a large extent the porosity and subsequently the strength of a mixture.

From tables 4.1 and 4.2, Grout C requires less water for mixing the same quantity of grout than Grout A and Grout B and has a higher compressive strength after both 7 days and 28 days curing in a moist room. However, the mean unit weight does not differ much from that of Grout B. Grout A was found to have a lower unit weight and a correspondingly lower compressive strength than the other two grouts. The lower unit weight could be assumed to imply that there may be more pore spaces within the hardened Grout A, on further assumption that similar materials were used in the proportioning of the grouts. This assumption was confirmed by the sorptivity plots shown in figure 4.1.

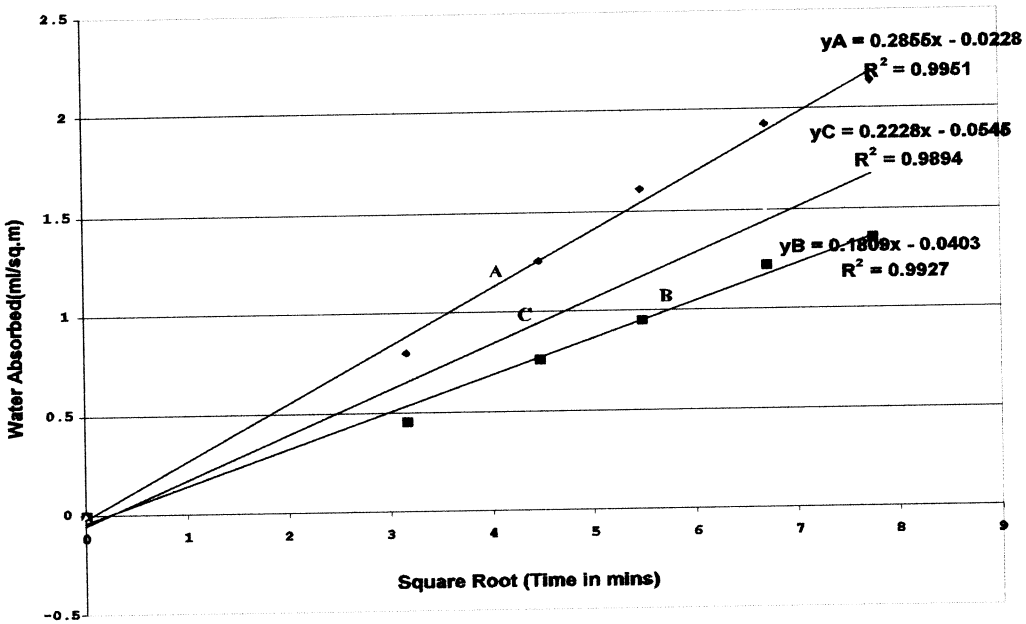

Figure 4.1 : Plot of Absorbed Water Vs. Square Root of Time

Grout A was found to have a higher sorptivity than the other two grouts.

Table 4.3 shows the summary results of the unit weight measurements, the compressive strength tests and the water absorption tests. From this table, grout type A, which has the lowest unit weight was found to have the highest water sorptivity of 0.2855 $ml/m^2/min^{1/2}$. Grout type B, which has the highest unit weight was found to have the lowest water sorptivity of 0.1809 $ml/m^2/min^{1/2}$.

Based on the results of the water sorptivity tests on the three grouts, grout type A, which was found to have the highest sorptivity of the three grout types and grout type B, which was found to have the lowest sorptivity were used in the construction of the base

plate arrangement test specimens for the corrosion tests to determine if the permeability of grouts is a factor in the corrosion of embedded anchor bolts and nuts in grouted lighting and sign structures.

Table 4.3: Summary of Test Results on Hardened Grout.

Grout Type	Unit Weight (pcf)	Compressive Strength (psi)	Sorptivity $ml/m^2/min^{1/2}$
A	127.32	8,198	0.2855
B	135.83	8,420	0.1809
C	135.75	9,223	0.2228

CHAPTER 5
RESULTS OF THE CORROSION TESTS

In this chapter , the results of the corrosion tests, namely, corrosion potential measurements, corrosion rate measurements, weight loss measurements and visual assessment on the base plate arrangement test specimens are presented and discussed.

5.1 Corrosion Potential Measurements

The corrosion potential of the anchor bolts in the base plate arrangements were measured at 4 hour intervals starting from the time the salt solution was drained off and continued throughout the time that the specimen remained dry. The duration of the various measurements (the time the specimen remained dry) was varied to obtain an understanding of the variations of the corrosion potential with various drying times of the specimens. The P-R monitor version 4.40C was extensively used for the corrosion potential measurements as described under section 3.5 because of its versatility (measures corrosion potential, corrosion rate, polarization resistance and solution resistance). The measurement periods (times when the specimens were kept dry) were varied during the various measurements to observe the trend of the electrochemical measurements over long periods as measurements obtained within the first 24 hours of drying was suspected to have been influenced by excessive moisture within the grouted arrangements.

The RPX1 corrosion transmitter was used to measure the corrosion potentials at 6 weeks and 8 weeks to confirm the trend of measurements obtained with the PR-Monitor. The corrosion of four embedded bolts was measured at the positions indicated in Figure 3.13.

Figures 5.1and 5.2 show the plots of corrosion potential measured with the PR-Monitor with time after 2 weeks and 4 weeks respectively. It can be seen that the systems with Grout A and Grout B showed more negative corrosion potential than the system with no grout. The magnitude of the negative potential decreased with drying time for all the three systems. The corrosion potentials for the Grout A and Grout B systems approach one another with drying time.

Figures 5.3 and 5.4 show the plot of corrosion potential measured with the RPX1 corrosion transmitter with time after 6 weeks and 8 weeks respectively. There was no significant difference observed in the trend of measured corrosion potential with time using the two instruments, the PR-Monitor was therefore used for the remaining measurements.

At the end of the 8th week, the three specimen in the dry tank were left to dry for ten days while electrochemical measurements were being made with the P-R monitor. The corrosion potentials are plotted in Figure 5.5. It can be seen that the corrosion potentials for the three systems approach one another as the samples dried out.

Figure 5.6 shows the same type of plot after 10 weeks, when the specimens which had been left to dry for 10 days after the 8th week measurements were soaked for only one hour period and left to dry again.

Figure 5.7 shows measurements within the 11th week after the dry specimens were soaked for only 30 minutes after the 10th week measurements.

Figure 5.8 shows the plot of corrosion potentials after two weeks daily wet-dry cycling of the salt solution after the 11th week measurements.

Variations in the length of the drying and soaking periods were made to understand the effects they might have on the electrochemical corrosion measurements. Appendix C shows the results of the individual test measurements on the anchor bolts. Measurements were not taken when the specimen were immersed in the salt solution to eliminate the effects of high moisture contents on the electrochemical measurements.

5.1.1 Discussion of Results of Potential Measurements

Figures 5.1 to 5.8 show that immediately after draining the salt solution, the potential of the arrangement was very negative for all the three specimens. The potential of the specimens with grout pads were however more negative, giving an indication that the zinc in the galvanized plate was contributing to the high negative potential as observed by Zhang and Valeriote (26). This high negative potential increased to less negative values with time when the moisture in the system reduced. After longer periods of drying, as indicated in Figures 5.5 through 5.8, the potential leveled off, with the potentials of the grouted specimens very close to but slightly lower than that of the specimen without grout. The difference was probably attributed to the presence of moisture within the grouts.

The corrosion potential of the system after 24 hours of drying was used to characterize the potential of the base plate arrangement when the moisture condition after wetting is considered stable enough.

The 24 hour period is considered representative of the wet and dry cycle of lighting and signing posts which is mainly caused by condensation of dew on the structure at night and drying during day time. Moreover, the foundation of the structure would not be moisture saturated in service except during occasional rains of long duration. The potential measurements at 24 hours after drying are plotted against time (in weeks) in Figure 5.9 .

From Figure 5.9, the corrosion potential of the base plate arrangement without a grout pad was found to lie within the limits of potentials for active corrosion for the entire period of measurement. The corrosion potential of the base plate arrangement with grout Type A as the material for grout pad started with values more negative than -700 mV after 2 weeks but assumed values within the observed corrosion potential of corroding steel after about 5 weeks of testing. The corrosion potential for the base plate arrangements with grout type B as material for the grout pad started with values more negative than -700 mV, but assumed values within the limits of active corrosion potentials of steel after about 9 weeks of testing.

These results gave an indication that throughout the period of testing, the anchor bolts in the base plate assembly without a grout pad experienced active steel corrosion, however, the corrosion of the anchor bolts in the assembly with a grout pad could not be ascertained because of the interference of the potential of the galvanized plate with the measurements, this condition resulted in more negative half cell potentials than normally obtained in such measurements in corroding steel.

5.2 Electrochemical Corrosion Rate Measurements

Figure 5.9 shows the plot of the corrosion rate measurements made with the P-R monitor version 4.40C against time in weeks. Even though measurements were obtained at various times after draining the salt solution from the specimen (Appendix D), the average corrosion rates after 24 hours of drying were used as explained in for the case of corrosion potentials in section 5.1.1.

The corrosion rate measurements obtained indicated that the corrosion rates of the embedded bolts and nuts within the grouted base plates were higher than the rates obtained for the base plate arrangement without a grout pad during testing periods when the corrosion potentials obtained from the potential measurements discussed under section 5.1 were more negative than -700 mV. However, during the periods when the measured potentials were within the limits of corrosion potentials for steel, the corrosion rates for the grouted base plates were found to be lower than the rates measured on the plate arrangements without a grout pad.

5.2.1 Problems With Corrosion Rate Measurements Using Linear Polarization Technique

Research results (26, 27) have shown the following reasons as sources of error in corrosion rate measurements using the linear polarization resistance technique.

1. Investigations (26,27) have shown good agreement between gravimetric and electrochemical measurements and that the values of B in the Stern and Geary Equation varies between 26 mV for active steel rebars and 52 mV for passive rebars depending on the state of corrosion of the rebar.

The value of "B" was assumed to be 35 mV, the correct value for B might be somewhat different, and this may be a source of error in the estimation of the corrosion rate measured.

2. Due to the effect of the corrosion of zinc in the galvanized plate, the anodic and cathodic Tafel slopes β_a and β_c in the Stern and Geary equation may differ considerably from those observed for the corrosion of steel. The 'B' value of 35 mV (for corroding steel) used in the configuration of the P -R monitor 4.40C may therefore not accurately characterize the corrosion rate of the anchor bolts embedded in the grouted base plate arrangements in the presence of the galvanized steel.

3 The positioning of the guard ring electrode in this research as shown in Figure 3.13 makes it difficult to determine the actual area of the embedded anchor bolt over which the electrical signal from the central guard ring electrode was concentrated. A larger area of concentration of the electrical signal on the embedded steel than the diameter of guard ring electrode will lead to the overestimation by the instrument (as D in equation 3.1 will be smaller). The determination of this area is very critical in the corrosion rate assessment as has been emphasized in various researches (18, 26 and 27). Also a guard ring electrode is normally placed directly over the corroding metals which usually has a thin cover.

4. Broomfield J. P (18) found out that high resistivity concrete, variations in potential and deep cover leads to errors in the current (corrosion rate) measurements using confined guard ring electrode.

The deep cover of the concrete over the steel bolt as used in this test set-up would lead to measurement errors.

The above complications, coupled with the fact that the guard ring electrode could not be placed directly over the embedded anchor bolts in the base plate arrangements made the corrosion rate measurements obtained with the P - R Monitor version 4.40C not very reliable in this project setup.

5.3 Visual Assessment

At the end of 14 weeks of wet - dry cycling, the base plates were dismantled and the grout pads of the grouted base plate specimens were cut open to reveal the anchor bolts. Figures 5.11, 5.12 and 5.13 show pictures of the anchor bolts in the specimen without grout pad, anchor bolts in the specimen with grout A as material for grout pad and those within the specimen with grout B as material for grout pad respectively. It was observed that there was no discernible rust on the anchor bolt lengths embedded in the two grouts whereas there was substantial rust observed at corresponding lengths on the anchor bolts in the base plate arrangement without grout pad.

Figures 5.14, 5.15 and 5.16 show pictures of the galvanized base plates without grout pad, with grout A as grout material for the pad and with grout B as grout material for the pad after the 14 weeks of wet - dry cycling respectively. There was more deposition of white zinc oxide on the base plate in the arrangement without a grout pad than observed on the two base plates from the arrangements with grout pads.

The zinc oxide deposition on the base plate from the arrangements with the more permeable grout material was however, observed to be slightly more than the deposition on the plate with less permeable grout material (Grout A) for the pad.

5.4 Weight Loss Measurements

After the visual assessments, the nuts were removed from each sample. Care was taken to ensure that rust materials which were removed during the unscrewing of the bolts were collected on a piece of paper. The weight of the rusted nuts between the annular base plate and the foundation concrete were then taken together with any rust removed during the unscrewing of the respective nut. Rust remaining on the nuts were then removed with a brittle wire brush in accordance with ASTM test specification G1 - 1991 as described under section 2.6.2. of this report. Table 5.1 shows the results of the weight loss measurements.

5.4.1 Analysis of Results of the Weight Loss Measurements

A one way analysis of variance (ANOVA) was performed to determine the significance of the effects of grouts, using the randomized block design with assembly type as treatment units and tank as block. Table 5.2 shows the results of the analysis. Table 5.2 gives an indication that there was no significant difference in the wight loss obtained between the two tanks, however, there was an indication that at least the mean weight loss of one of the specimen is different from the others.

Table 5.1 Results of the Weight Loss Measurements.

Bolt Number	Weight Loss (grams)					
	Tank 1			Tank 2		
	Grout A	Grout B	No Grout	Grout A	Grout B	No Grout
1	0.05	0.02	0.62	0.03	0.07	0.67
2	0.04	0.08	0.42	0.10	0.09	0.73
3	0.00	0.05	0.43	0.03	0.12	0.63
4	0.07	0.04	0.89	0.09	0.05	0.52
5	0.04	0.06	0.65	0.06	0.10	0.55
6	0.03	0.03	0.58	0.04	0.09	0.62
7	0.02	0.05	0.85	0.05	0.08	0.63
8	0.03	0.02	0.65	0.03	0.06	0.60
Mean	0.04	0.04	0.64	0.05	0.08	0.62
standard deviation	0.02	0.02	0.17	0.03	0.022	0.07
coeff. of variation	0.59	0.47	0.27	0.52	0.27	0.11

Table 5.2 ANOVA Table for The Weight Loss Measurements.

Source	DF	SS	MSE	F	Pr> F	sig. diff at 5% level ?
Grout	2	3.514	1.750	303.53	0.0001	Yes
Tank	1	0.002	0.002	0.370	0.5469	No
Error	44	0.255	0.006			
Total	47	3.771				

In view of the outcome of the analysis of variance, further analysis was carried out using Duncan's multiple range test procedure. The outcome of this multiple comparison test (Table 5.3) showed that there was no significant difference between the mean weight losses measured on the two base plate assemblies with grout pads using grouts A and B, but the mean measured weight loss on the base plate assembly without a grout pad differs significantly from the measurements on the two assemblies with grout pads.

Table 5.3 Multiple Comparison Results of Weight Loss Measurements (Duncan's)

CONDITION	Mean Weight Loss	Grouping
Grout A	0.044	A
Grout B	0.063	A
No Grout	0.628	B

Means with the same letter are not significantly different at the 5% level($\alpha = 0.05$).

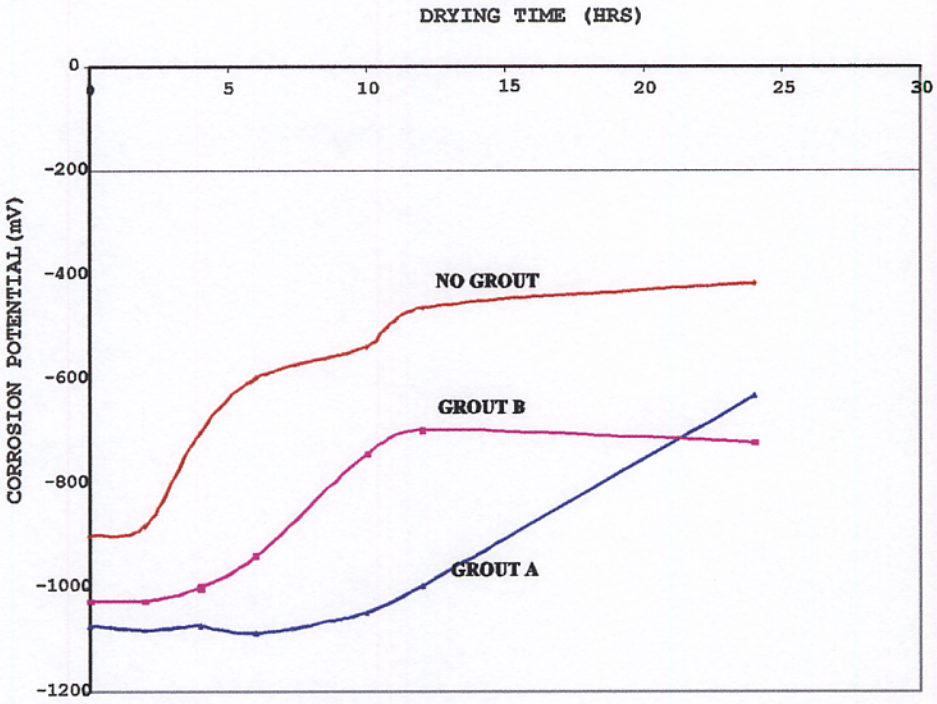

FIGURE 5.1 : CORROSION POTENTIAL VS. DRYING TIME AFTER 2 WKS.

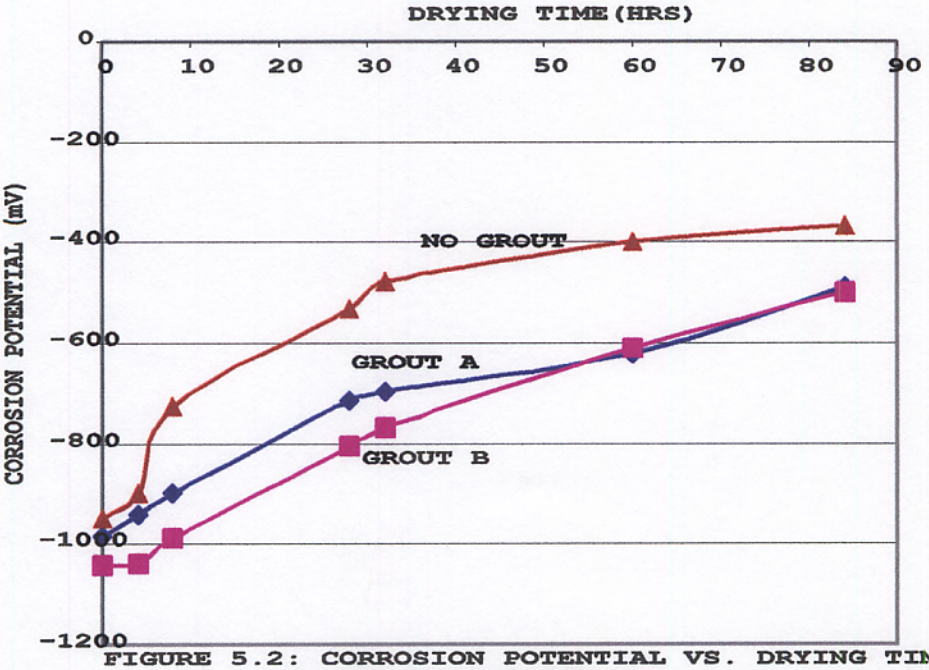

FIGURE 5.2: CORROSION POTENTIAL VS. DRYING TIME
4 WKS AFTER START DATE

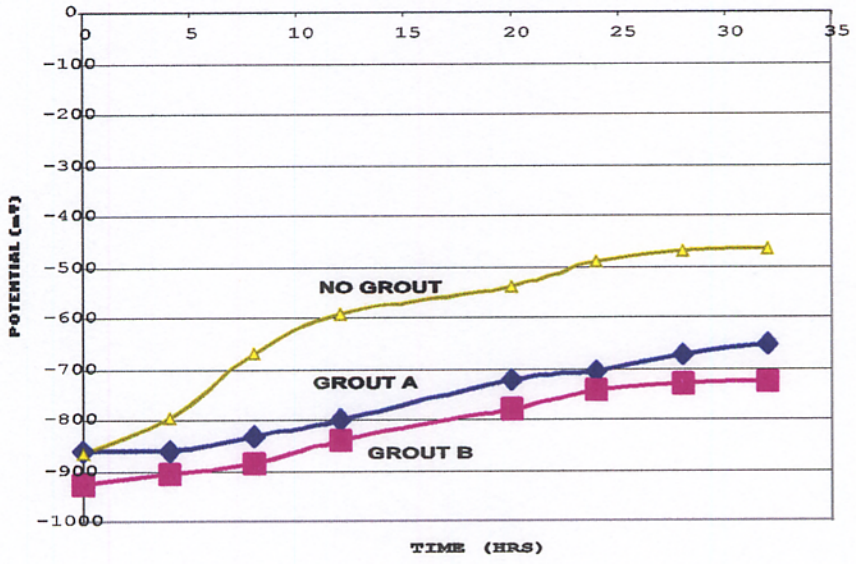

Figure 5.3: Corrosion Potential Measurements after 6 Weeks (With RPX1)

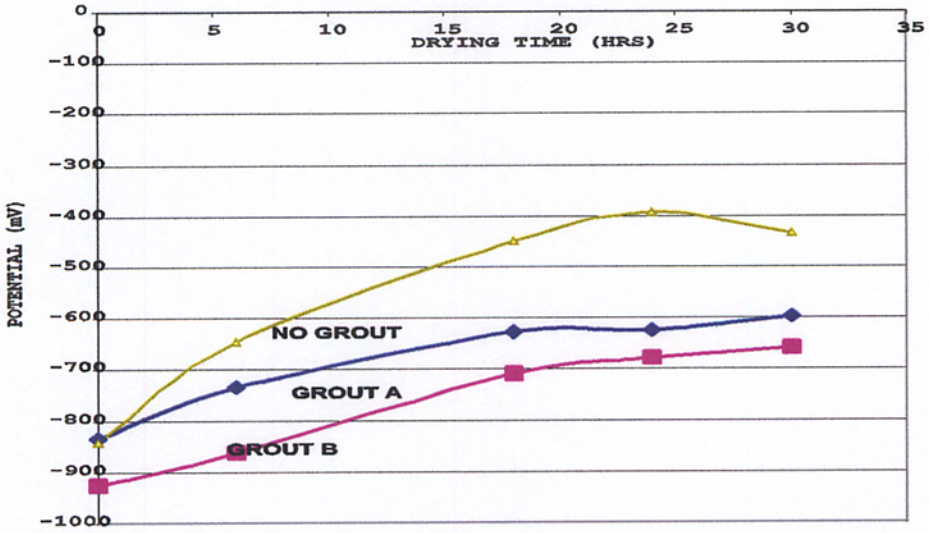

Figure 5.4: Corrosion Potential Measurements after 8 Weeks (With RPX1)

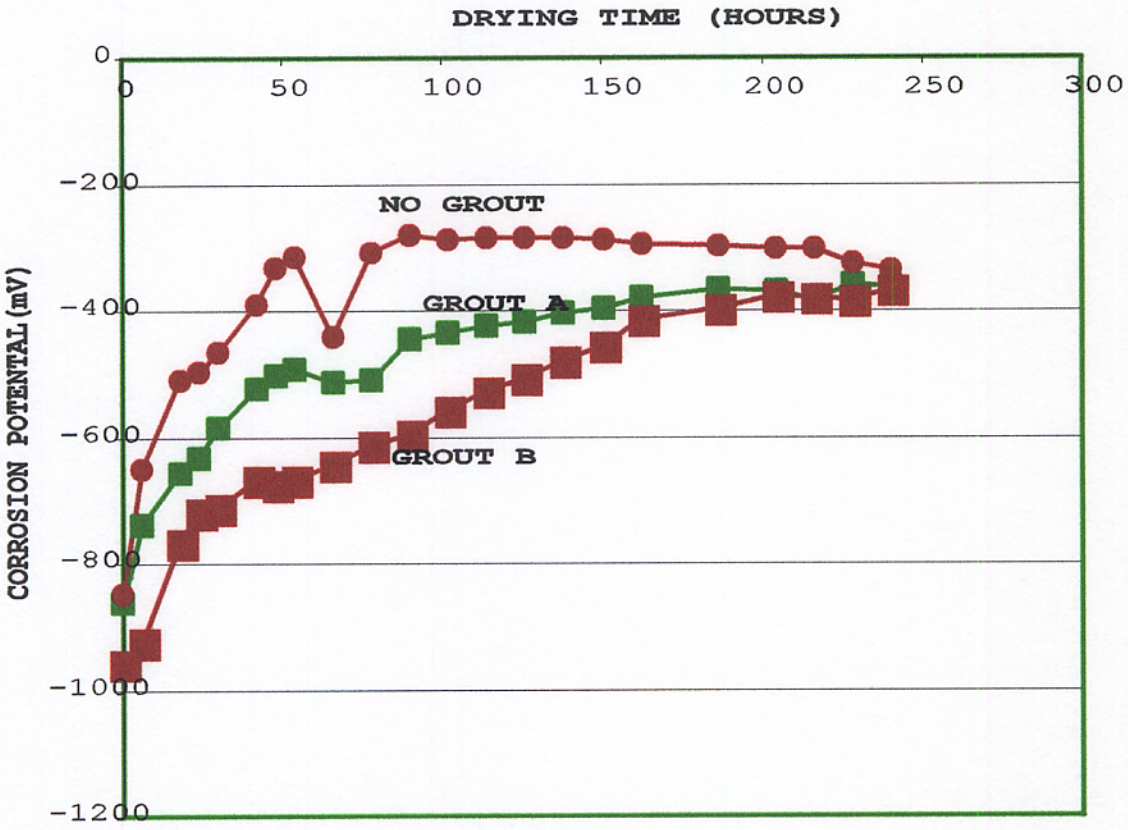

Figure 5.5: Corrosion Potential Vs. Drying Time (After 8 Weeks) Using P-R Monitor

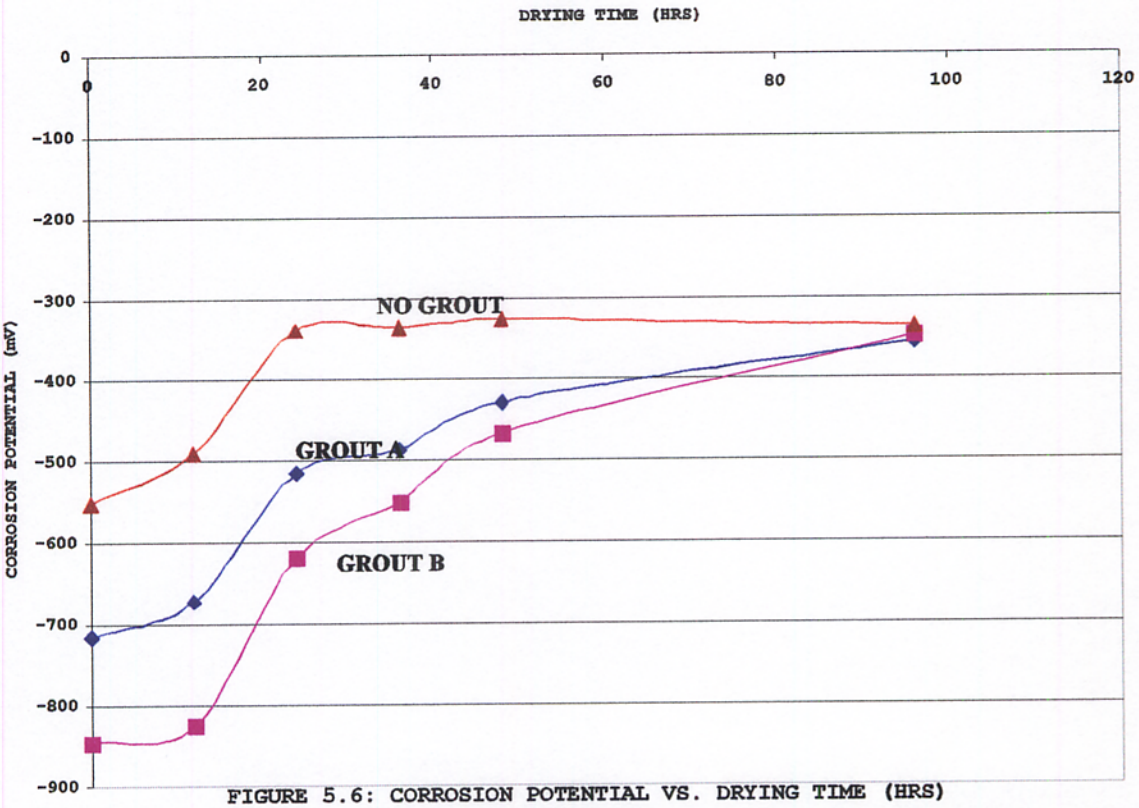

FIGURE 5.6: CORROSION POTENTIAL VS. DRYING TIME (HRS)
AFTER 1HR SOAKING (10 WKS AFTER START DATE) WITH P-R MONITOR

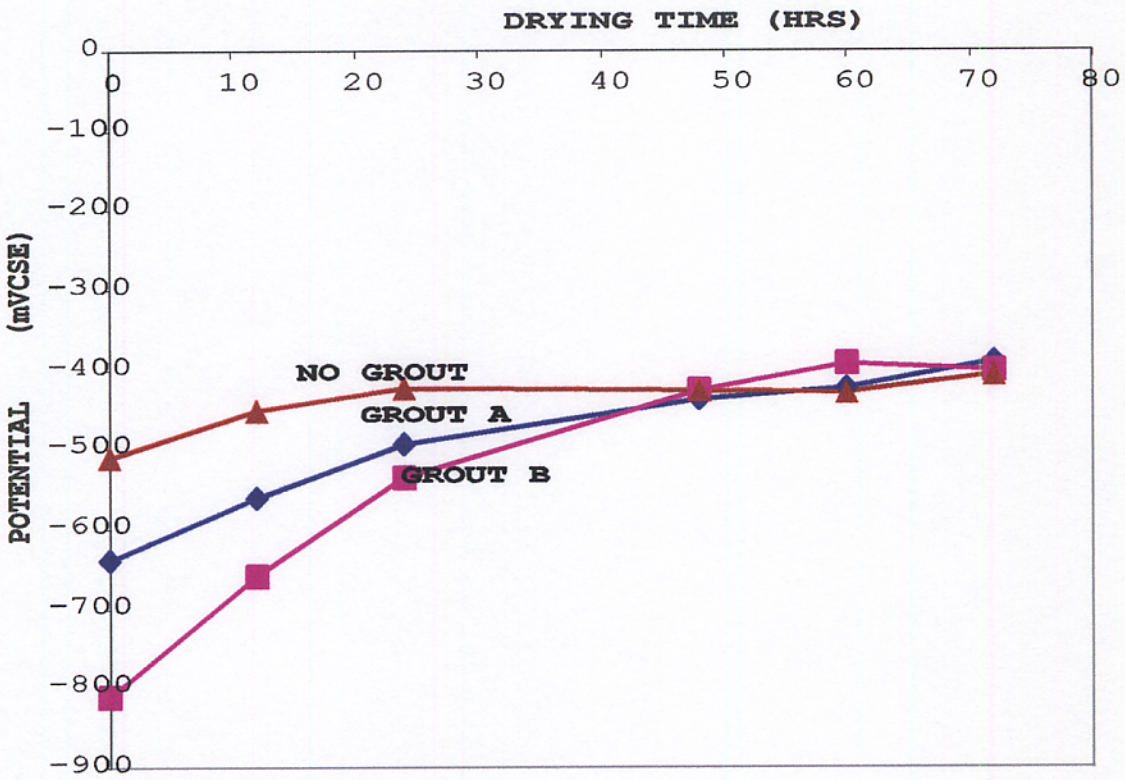

Figure 5.7: Corrosion Potential Vs. Drying Time with Pr-Monitor (30 Minutes Soaking, 11 Weeks after Start Date)

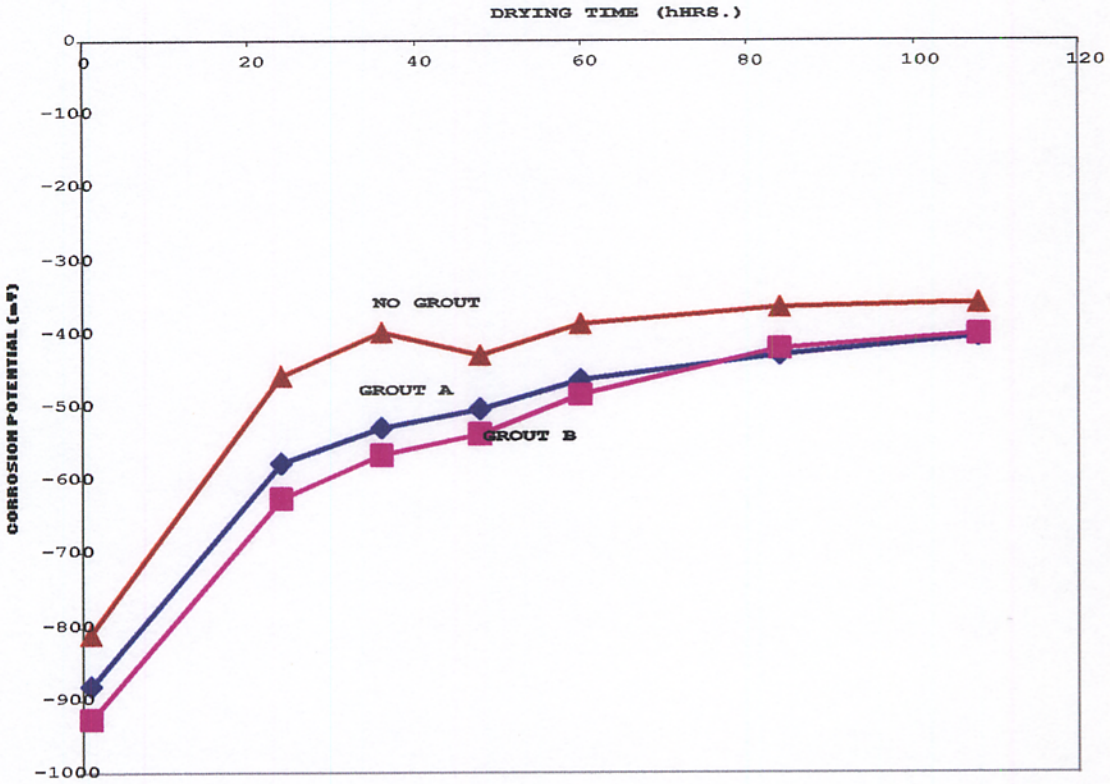

Figure 5.8 : Corrosion Potential Vs. Drying Time13 Weeks after Start

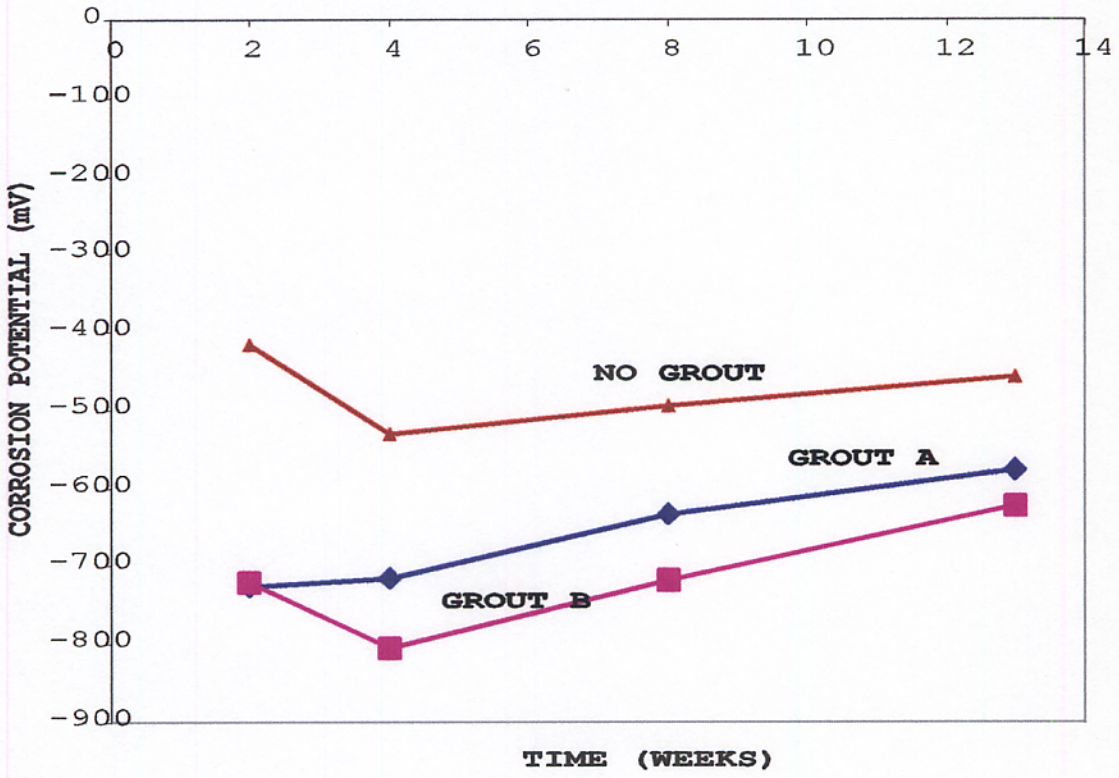

Figure 5.9 : Corrosion Potential Vs. Time (Weeks)

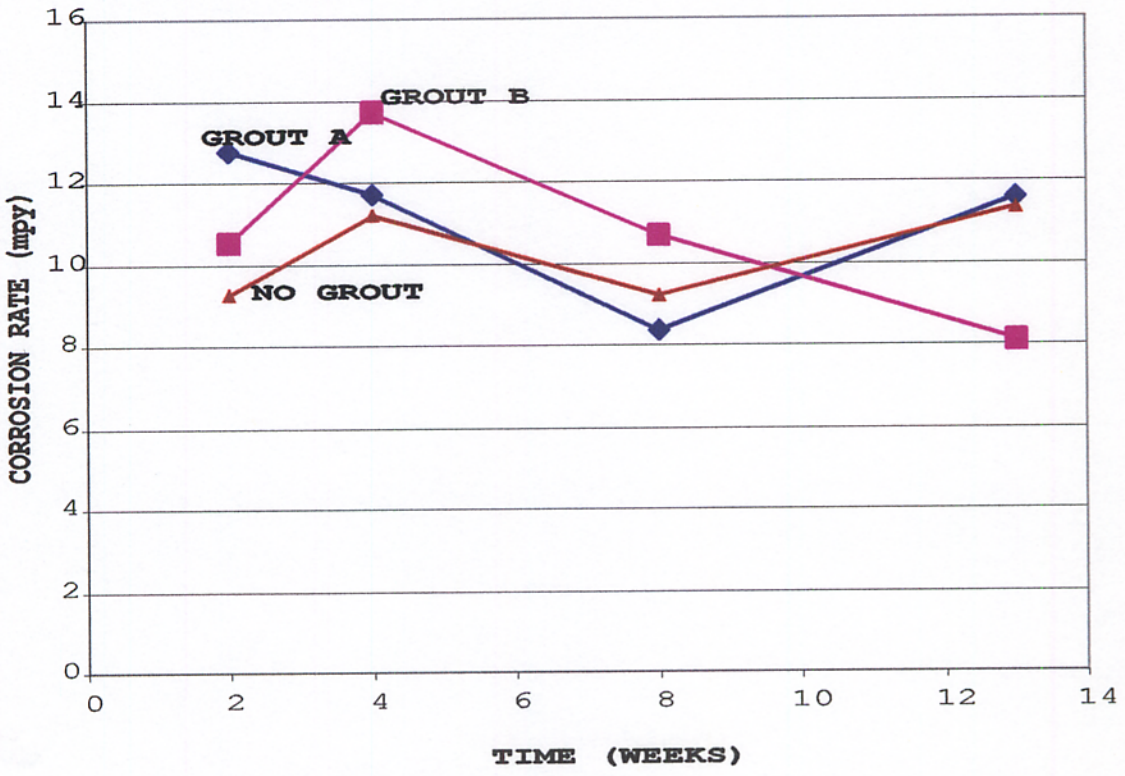

Figure 5.10: Corrosion Rate Vs. Time in Weeks

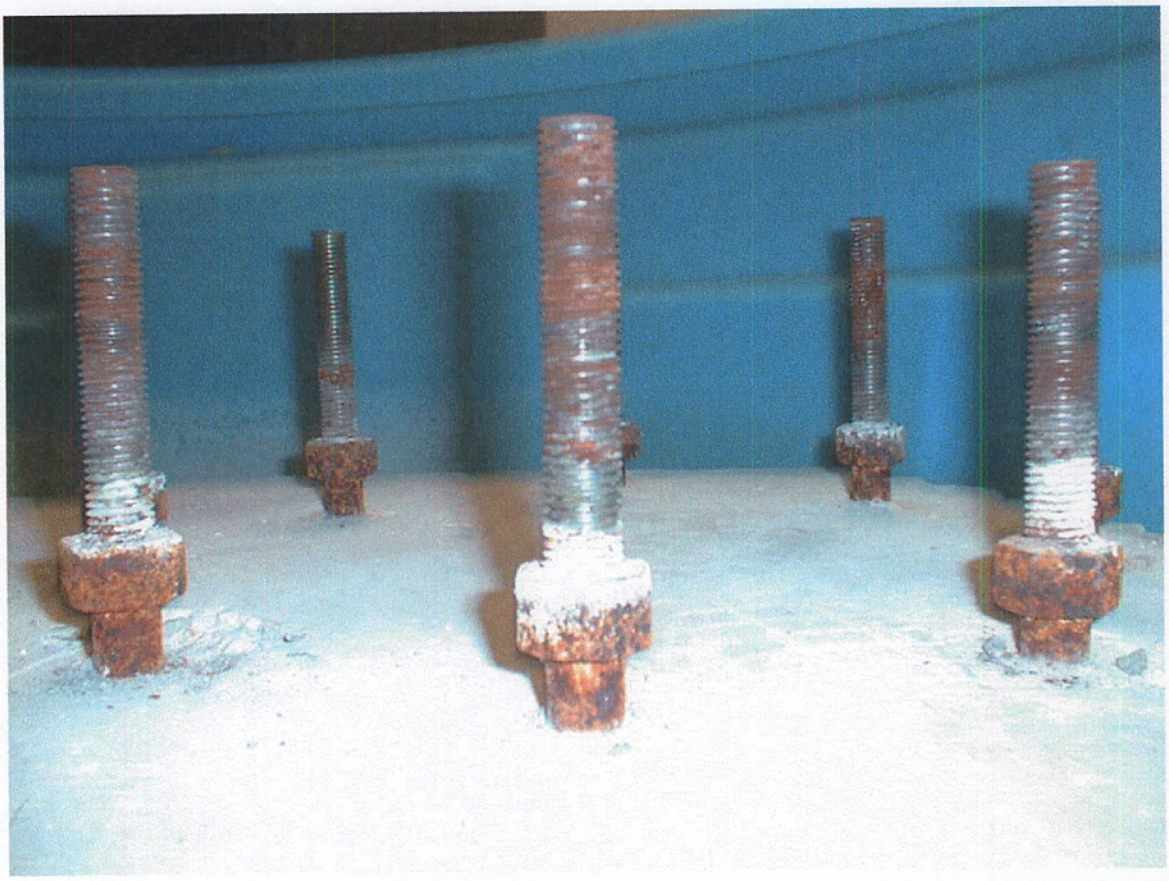

Figure 5.11: Picture Of Anchor Bolts In Base Plate Arrangement Without A Grout Pad After 14 Weeks Of Wet – Dry Cycling Of Salt Solution

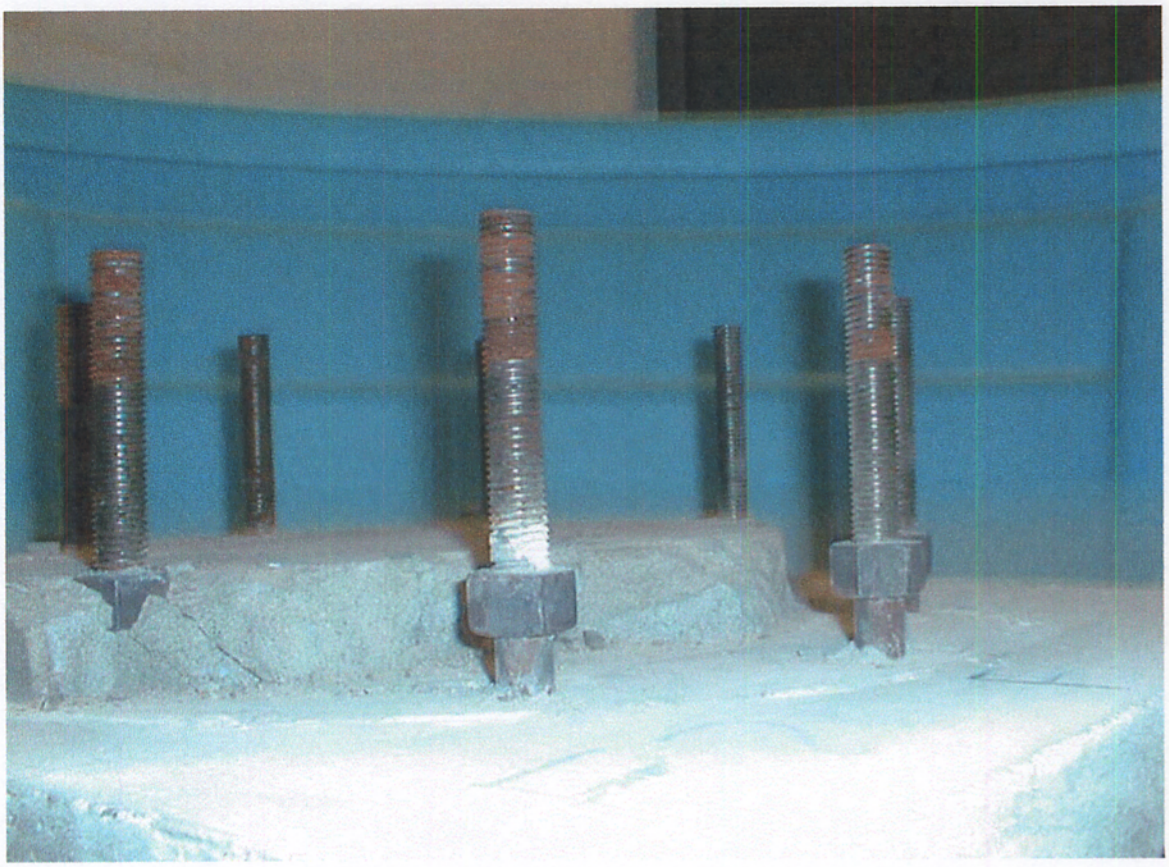

Figure 5.12: Picture of Anchor Bolts in Base Plate Assembly With Grout Type A for Grout Pad After 14 Weeks of Daily Wet-Dry Cycling of Salt Solution

Figure 5.13 : Picture Of Anchor Bolts In Base Plate Arrangement With Grout B Material As Grout Pad After 14 Weeks Of Wet – Dry Cycling Of Salt Solution.

Figure 5.14 : Picture Of Galvanized Plate From Base Plate Arrangement With Out Grout Pad After 14 Weeks

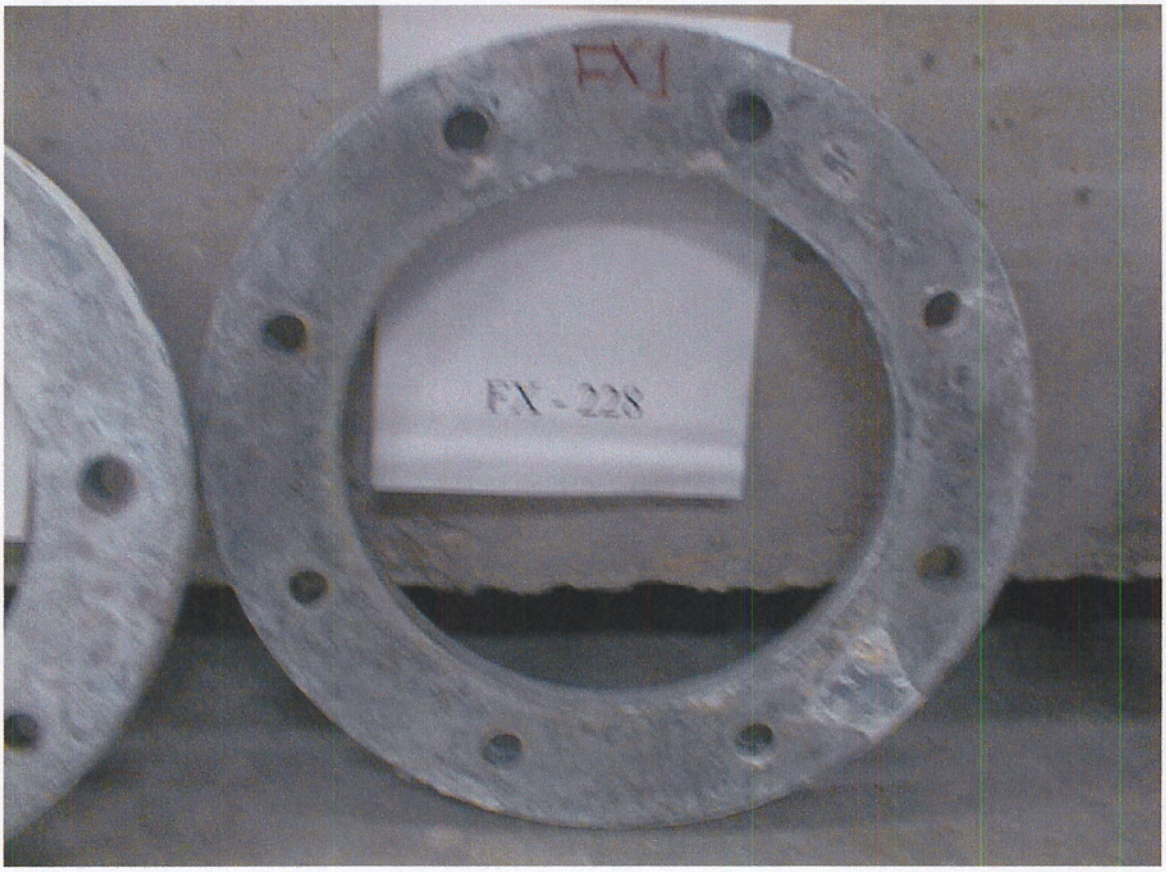

Figure 5.15: Galvanized Base Plate From Arrangement With Grout A As Grout Material For Grout Pad

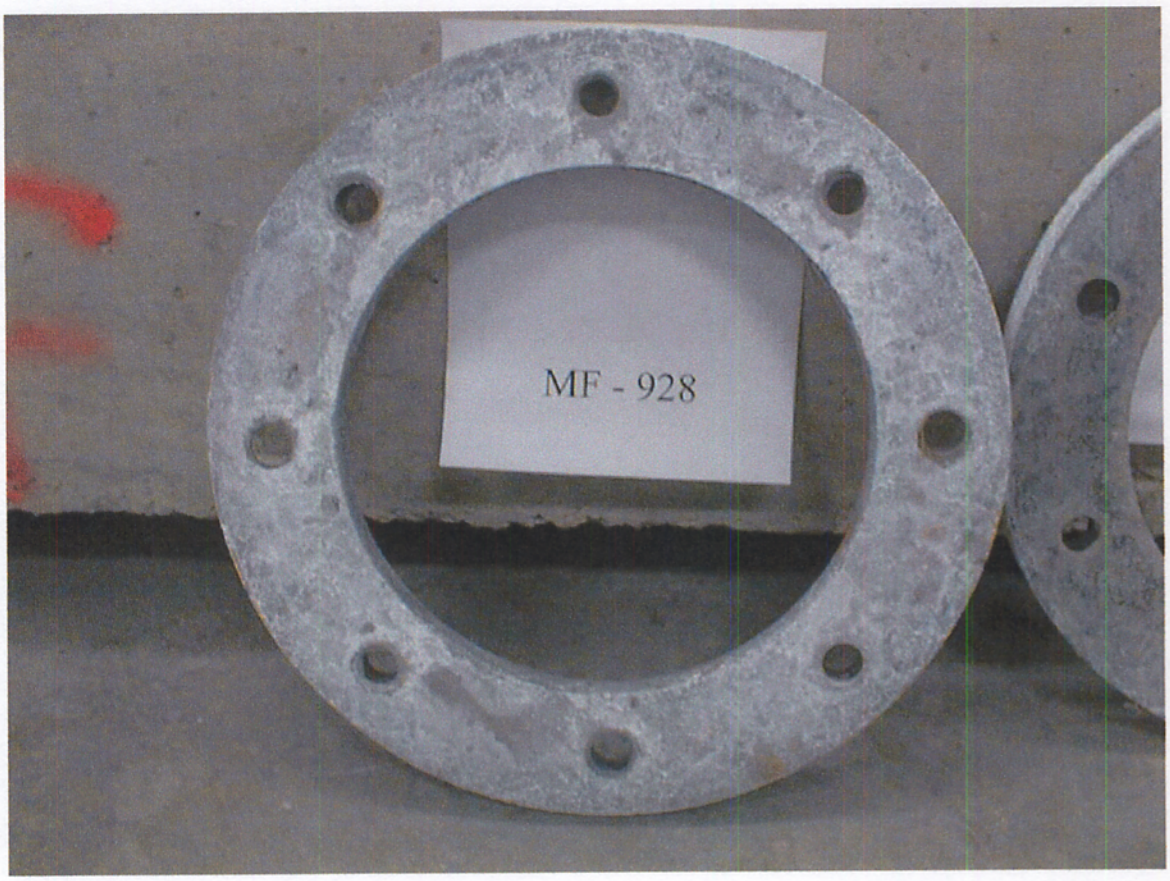

Figure 5.16 : Picture Of Galvanized Plate From Base plate Assembly With Grout B as Material For Grout Pad After 14 Weeks

CHAPTER 6
SUMMARY, CONCLUSIONS AND RECOMMENDATIONS

6.1 Summary of Corrosion Measurements

The durability of grouted annular base plate assemblies for tubular high mast poles, roadway light poles, and traffic mast arms connected to a concrete foundation have been a matter of concern to the Florida DOT. The corrosion of embedded bolts, nuts and the annular base plates in the presence of water, oxygen and aggressive ions such as chlorides have been determined to affect the durability of the structures.

Measurements of the corrosion of the embedded bolts and nuts in two grouted base plate assemblies, one with a grout of high water absorption rate(Grout Type A) and the other with a lower water absorption rate (Grout Type B) have been made and compared with the corrosion of bolts and nuts in similar base plate arrangements without a grout pad. Three methods of measurements, namely 1) electrochemical methods, 2) weight loss techniques, and 3) visual assessment method were used for the measurements. The foregoing are the results of the corrosion measurements.

6.1.1 Electrochemical Measurements

Due to the effects of the galvanized base plates on the electrochemical measurements made in this study, comparison of the results obtained for the three base plate assemblies could not be made.

The visual assessment and the weight loss techniques were therefore used to assess the differences in the performance of the three specimens.

6.1.2 Visual Observations and Weight Loss

The observations made during the visual assessment and weight loss measurements complemented each other. The embedded length of the anchor bolts in the base plate arrangements test specimen without grout pad showed extensive rust formation while there was only a little rust on the embedded length of the anchor bolts in the base plate arrangements test specimens with grout pads.

While the mean weight loss of the embedded nuts in the grout pad with the more permeable material (A) was slightly less than the loss from the embedded nuts in the grout pad with the less permeable grout (B), the difference was statistically insignificant.

The visual observation also show more loose white zinc oxide on the galvanized base plate in the assembly without a grout pad than observed on the assemblies with grout pads, indicating that there was more corrosion of the base plate due to exposure to the atmosphere. There was also slightly more deposition of the white zinc oxide on the base plate of the grout pad with the less permeable grout material than on the plate on the arrangement with the more permeable grout material for the pad.

The slight difference in the observations on the two grouted assemblies may be explained by the fact that with the test conditions, both base plate arrangements become saturated during the time that the assembly is submerged.

The total corrosion of the embedded metals therefore will depend on the time that the grout will take to become completely dry. The assembly with a grout pad of the less permeable grout material will obviously retain water for a longer period and hence more corrosion will be observed. These observations were in agreement with both the potential and weight loss measurements.

6.1.3 Effect of Water Absorption Rate of Grout on Corrosion of Anchor Bolts

The permeability of the grout cover to the anchor bolts were characterized by the water absorption rate. Grout A was found to have a higher sorptivity of 0.286 $ml/cm^{-2}/min^{1/2}$ and Grout B had a low sorptivity of 0.181 $ml/cm^{-2}/min^{1/2}$. From the visual observations and the weight loss measurements, it was observed in this study that a grout with higher permeability will protect the anchor bolts in the base plate arrangement better than grouts with lower permeability under the severe conditions of testing adopted in this project. This would be true only if the grout pads are completely submerged for a long period of time, become saturated and moisture gets to the embedded bolts. The reverse is otherwise true. The statistical analysis however indicated that there is no significant difference in the corrosion protection of the embedded bolts by the two grouts.

6.2 Conclusions

The results of this investigation show that;

1) The use of grout pad under signing and lighting poles offers protection of both the embedded metals and base plate of the assembly.

The results of the weight loss measurements show that the corrosion of the anchor bolts and nuts in the assembly without a grout pad was of the order of about 10 times the corrosion in the assembly with a grout pad. Also, there is protection of the annular base plates by the use of grouts. The problem of maintenance of the base structures is therefore highly minimized with the introduction of grout pads.

2) Corrosion of the embedded anchor bolts in the base plate assemblies could not be effectively monitored with the electrochemical measurements using the linear polarization resistance technique with the guard ring electrodes as in the P-R monitor version 4.40C. Difficulty in positioning the guard ring electrode directly over the bolts, presence of varying moisture contents in the different test specimen configurations and the presence of the effect of zinc made the half cell corrosion potentials and corrosion rates measured in this project not quite reliable and therefore could not be used as a basis of comparison of the three different arrangements.

3) The statistical analysis of corrosion measurements by the weight loss technique shows that there is no significant difference in the protection offered by different grouts used in this study.

6.3 Recommendations

1) Grout pads are recommended for use under signing and lighting structures as they significantly reduce the maintenance requirements of the structure.

2) The water sorptivity test described in this project, is a simple test which can be used to determine the permeability of hardened grouts for acceptance and use for the grouting of base plates for signing and lighting posts to control the ingress of aggressive ions and prevent the corrosion of the embedded anchor bolts and nuts.

3) There is a need to conduct similar research on a number of the grouts approved by the Florida Department of Transportation for grouting of base plates for signing and lighting posts to correlate water sorptivity with corrosion activities so as to set limits of sorptivity or permeability requirements of grouts for signing and lighting posts.

4) The use of the linear polarization resistance technique to measure the rate of corrosion of the anchor bolts need to be reviewed in view of the presence of the effect of galvanized plates and the difficulty in positioning the guard ring electrode directly over the corroding anchor bolts. The macrocell technique, whereby an inert electrode is inserted in the grouted base plate arrangement to monitor corrosion rates could be reviewed and adopted in measuring the corrosion rate.

APPENDIX A
RESULTS OF TESTS ON HARDENED GROUTS

Table A1 : Measurements For Unit Weights

	Weight of Cubes (gm)		
Sample	1	2	3
Fx -228	278.4	289	282.9
Masterflo	290.5	285	299.9
Sika	282.5	286.4	288.1

Table A2: Unit Weights

Sample	1	2	3	Average	STD
Fx -228	128.29	129.14	124.52	127.32	2.4549
Masterflo	133.86	135.43	138.19	135.83	2.1929
Sika	134.24	136.1	136.91	135.75	1.3644

Table A3: Failure Loads in the Compressive Strength Tests

Sample	1	2	3	Average	STD
Fx -228	30,780	30,070	29,660	30170	566.66
Masterflo	28,730	31,600	30,240	30190	1435.7
Sika	32,210	31,680	31,600	31830	331.51

Table A4:Compressive Strengths (psi) - 7 Days

Sample	1	2	3	Average	STD
Fx -228	7,695	7,518	7,415	7542.5	141.66
Masterflo	7,183	7,900	7,560	7547.5	358.91
Sika	8,053	7,920	7,900	7957.5	82.878

Table A5: Failure Loads (lbs) - 28 Days

Sample	1	2	3	Average	STD
Fx -228	32,830	32,780	32,760	32790	36.056
Masterflo	33,380	34,760	32,900	33,680	965.61
Sika	37,900	36,120	36,650	36890	913.95

Table A6: Compressive Strengths (psi) - 28 Days

Sample	1	2	3	Average	STD
Fx -228	8,208	8,195	8,190	8197.5	9.0139
Masterflo	8,345	8,690	8,225	8420	241.4
Sika	9,475	9,030	9,163	9222.5	228.49

STD = STANDARD DEVIATION

APPENDIX B
RESULTS OF CALCULATIONS FOR ABSORPTION RATE MEASUREMENTS

Table B1: Measured Weights of Specimen in Grams

SAMPLE	FX -228		Masterflow - 928		SIKA - 220	
TIME(min)	1	2	1	2	1	2
0	1818.8	1772.1	1801.1	1786.7	1815.9	1818
10	1824.9	1778.9	1804.6	1790.6	1819.8	1822.8
20	1828.3	1782.9	1806.8	1793.3	1822.7	1826.2
30	1831	1785.9	1808.3	1794.9	1824.7	1828.6
45	1833.6	1788.5	1810.4	1797.1	1827.1	1831
60	1835.2	1790.3	1811.5	1798.2	1828.4	1832.2

Table B2: Weight of Water Absorbed in Grams

SAMPLE	FX -228		Masterflow - 928		SIKA - 212	
TIME(min)	1	2	1	2	1	2
0	0	0	0	0	0	0
10	6.1	6.8	3.5	3.9	3.9	4.8
20	9.5	10.8	5.7	6.6	6.8	8.2
30	12.2	13.8	7.2	8.2	8.8	10.6
45	14.8	16.4	9.3	10.4	11.2	13
60	16.4	18.2	10.4	11.5	12.5	14.2

Table B3: Mean of Absorbed Water/Area of Grout

SQRT(TIME)	FX	MF	SIKA
0	0	0	0
3.1623	0.798	0.4578	0.5382
4.4721	1.2558	0.7609	0.9279
5.4772	1.6084	0.9527	1.2001
6.7082	1.9301	1.2187	1.497
7.746	2.1404	1.3547	1.6517

APPENDIX C
RESULTS OF ELECTROCHEMICAL CORROSION MEASUREMENTS

TABLE C1: MEASUREMENTS USING THE PR - MONITOR AFTER 2 WEEKS

DRYING TIME		FX - 228		MASTERFLOW -928		NO GROUT	
DAYS	HOURS	Ecorr	RATE	Ecorr	RATE	Ecorr	RATE
1	0	-1072.7	20.47	-1026.9	24.67	-905.7	15.44
		-1072.3	21.72	-1026.3	26.55	-903.6	21.23
		-1071.7	21.57	-1025.3	26.63	-897.4	16.57
		-1071.4	24.24	-1024.9	23.86	-895.4	21.24
	2	-1082.8	11.38	-1025.8	20.19	-881.6	11.38
		-1082.2	14.74	-1025.4	19.69	-881	14.74
		-1081.2	14.05	-1024.6	21.55	-881.8	14.05
		-1080.8	15.53	-1024.1	19.22	-880.1	15.53
	4	-1074.3	41.2	-1000.5	18.04	-713.7	8.1
		-1073.7	35.4	-1000.9	17.37	-702.9	11.56
		-1073	37.82	-999.9	18.2	-696.5	7.89
		-1072.8	33.65	-999.5	17	-693.1	10.48
	6	-1088.9	17	-942.3	13.71	-602.1	11.12
		-1088.7	18.49	-939.7	17.7	-599.7	13.86
		-1087.9	14.9	-936.2	14.92	-595	11.74
		-1087.2	16.39	-934.7	17.38	-593	14.32
	10	-1049.7	22.48	-746.4	10.51	-533.2	8.49
		-1053	25.49	-744.8	13.03	-535.1	7.85
		-1053.5	15.11	-740.9	11.77	-540.2	8.09
		-1036.8	23.67	-739.3	13.05	-541.9	8.09
	12	-998.5	20.8	-699.2	11.77	-463.4	9.4
		-997.3	21.6	-698.3	12.01	-462.8	9.01
		-994.9	22.17	-696.2	11.91	-462.3	9.61
		-993.8	23.4	-695.1	11.91	-461.8	8.99
2	24	-633.1	14.74	-718.2	11.06	-413.9	7.21
		-629	14.19	-723.1	11.27	-414.1	7.21
		-632.1	14.62	-722.32	11.36	-418.3	7.33
		-630	14.31	-718.33	10.97	-409.7	7.09

TABLE C2: AVERAGES OF MEASUREMENTS IN TABLE C1

DRYING TIME		FX - 228		MASTERFLOW -928		NO GROUT	
DAYS	HOURS	Ecorr	RATE	Ecorr	RATE	Ecorr	RATE
1	0	-1072.03	22	-1025.85	25.4275	-900.525	18.62
	2	-1081.75	13.925	-1024.98	20.1625	-881.125	13.925
	4	-1073.45	37.0175	-1000.2	17.6525	-701.55	9.5075
	6	-1088.18	16.695	-938.225	15.9275	-597.45	12.76
	10	-1048.25	21.6875	-742.85	12.09	-537.6	8.13
	12	-996.125	21.9925	-697.2	11.9	-462.575	9.2525
2	24	-631.05	14.465	-720.65	11.165	-414	7.21

TABLE C3: MEASUREMENTS USING THE PR - MONITOR
AFTER 4 WEEKS

DRYING TIME	FX - 228		MASTERFLOW -928		NO GROUT	
HOURS	Ecorr	RATE	Ecorr	RATE	Ecorr	RATE
0	-984.9	26.71	-1050.5	27.71	-964.1	17.33
	-984.4	26.73	-1045.4	26.98	-958.2	17.49
	-984.1	26.29	-1039	28.51	-933.2	16.7
	-983.8	26.48	-1039.1	27.75	-932.4	17.4
4	-951.7	14.64	-1031.2	21.73	-899.3	19.46
	-950	14.58	-1033.5	14.35	-920.3	21.04
	-947.2	17.5	-1041.2	17.5	-870.8	18.3
	-920.3	17.04	-1041.6	18.22	-871.5	18.85
8	-901.4	20.33	-1011	21.44	-729.8	18.4
	-909.3	21.29	-979.9	15.12	-717.4	21.74
	-895.3	17.59	-978.3	16.43	-688.6	11.81
	-891.9	20.32	-979.7	15.59	-773.2	8.83
28	-720.6	12.01	-824.1	16.72	-501.8	11.11
	-717.3	11.68	-825.3	15.78	-500.8	11.25
	-706.6	12.05	-783.3	12.94	-522.1	10.84
	-712.8	11.39	-782.8	12.14	-598.6	11.06
32	-702.9	14.14	-779.1	13.34	-475	11.83
	-699.2	14.07	-778.9	12.78	-530.9	11.82
	-694	14.75	-747.3	10.58	-452.7	11.86
	-692.4	12.83	-771.4	11.41	-450	9.84
40	-687.4	11.44	-731.6	11.74	-408.9	9.27
	-698.9	8.91	-730.5	11.56	-408.5	9.22
	-570.8	11.93	-711.5	11.11	-423.5	10.15
	-570	12.53	-711.6	11.03	-500.5	9.57
60	-621.4	11.84	-610.9	10.9	-397.6	8.48
84	-488.9	8.91	-500.6	8.86	-366.5	6.33

TABLE C4:AVERAGES OF MEASUREMENTS IN TABLE C3

DRYING TIME	FX - 228		MASTERFLOW -928		NO GROUT	
HOURS	Ecorr	RATE	Ecorr	RATE	Ecorr	RATE
0	-984.3	26.5525	-1043.5	27.7375	-946.975	17.23
4	-942.3	15.94	-1036.88	16.69	-896.8	19.4125
8	-899.475	19.8825	-987.225	17.145	-727.25	15.195
28	-714.325	11.7825	-803.875	14.395	-530.825	11.065
32	-697.125	13.9475	-769.175	12.0275	-477.15	11.3375
60	-621.4	11.84	-610.9	10.9	-397.6	8.48
84	-488.9	8.91	-500.6	8.86	-366.5	6.33

TABLE C5:MEASUREMENTS USING THE PR - MONITOR
AFTER 8 WEEKS

DRYING TIME		FX		MF		NO GROUT	
DAYS	HOURS	Ecorr	RATE	Ecorr	RATE	Ecorr	RATE
1	0	-862.6	16.66	-966.4	18.77	-855.1	21.97
		-860.9	21.29	-949.5	20.79	-841.4	23.92
		-862.2	18.72	-945.3	19.57	-842.3	22.33
		-891.3	19.17	-970.6	19.57	1854.2	22.55
	6	-744.8	3.66	-924.5	11.47	-665	6.7
		-738.5	10.89	-920.2	15.64	-663.2	17.09
		-730.9	14.94	-920.35	10.55	-617	14.84
		-738.1	9.83	-924.35	16.56	-648.4	12.88
	12						
	18	-662.6	10.41	-766.9	10.42	-585.6	10.6
		-652.5	8.07	-772.9	11.22	-547.4	10.76
		-673.4	4.21	-753.4	7.34	-477.7	10.87
		-642.9	8.74	-767.5	8.9	-423.4	10.49
2	24	-676.7	2.65	-748.8	8.38	-533.8	8.95
		-615.6	6.44	-686.7	11.93	-498.6	9.35
		-604.4	13.18	-720.7	9.39	-453.8	9.36
		-632.4	7.42	-754.9	13.05	-495.4	9.22
	30	-546.6	17.08	-713.8	28.47	-388.7	28.73
		-598.8	6.37	-736.2	32.27	-559.9	3.2
		-608.5	7.49	-680.8	9.8	-449.9	8.21
		-584.7	10.31	-710.3	23.52	-466.2	13.38
	42	-455.8	10.65	-672.8	9.5	-386.2	4.64
		-458.4	8.99	-584.3	10.98	-390.6	9.71
		-624.8	3.93	-710.6	9.73	-482.4	4.83
		-553.2	8.89	-698.9	9.25	-299.7	5.55
3	48	-516.3	6.9	-693.3	9.4	-316.9	5.38
		-475	7.41	-631	3.33	-315.4	6.63
		-526.5	7.2	-691.4	8.75	-318.6	5.85
		-495.4	9.84	-677	7.33	-369.8	8.22
	54	-493.4	6.38	-678.2	9.7	-311.7	5.34
		-457.3	6.22	-682.2	9.04	-314.6	6.52
		-498.1	8.32	-663.1	7.43	-319.4	5.4
		-519.5	7.48	-643	4.35	-316.4	5.47

TABLE C5 Continued: MEASUREMENTS USING THE PR - MONITOR AFTER 8 WEEKS

D RYING	TIME	FX - 228		MASTERFLOW -928		NO GROUT	
DAYS	HOURS	Ecorr	RATE	Ecorr	RATE	Ecorr	RATE
3	66	-552.9	4.74	-647.7	7.66	-440.8	6.78
		-475.3	6.21	-648.6	8.8	-429.4	8.28
		-545.2	9.15	-628.8	9.07	-453.4	7.67
		-518.6	9.21	-642.1	9.27	-438.2	6.42
4	78	-545.5	8.23	-601.7	8.22	-336.7	4.74
		-499.1	7.1	-605.6	7.32	-287	6.3
		-482.7	6.1	-630.7	7.93	-278.1	4.88
		-509.3	7.55	-612.4	6.95	-326.5	3.31
	90	-449.7	4.87	-584.1	8.55	-276.1	4.74
		-416.7	5.19	-590.2	7.16	-284.6	5.73
		-446.3	8.17	-608	7.38	-276.7	4.45
		-468.2	7.06	-596.3	6.48	-284.5	3.73
5	102	-439.6	4.91	-559.1	6.44	-281.9	4.62
		-406.5	5.4	-546.9	6.86	-289.9	5.08
		-434.5	6.93	-547.7	6.7	-284.8	4.75
		-460.1	7.83	-571.9	7.47	-286	3.46
	114	-423.5	4.89	-526.3	6.42	-279.3	3.86
		-398.9	6.24	-515.1	7.58	-288.6	5.24
		-428.6	6.7	-517.2	7.27	-279	3.88
		-438.7	6.78	-546.1	6.69	-282.8	3.83
6	126	-442	7.72	-513.8	5.83	-285.6	6.78
		-390.8	6.28	-489.5	6.19	-279.5	4.22
		-412.4	4.93	-497.4	6.62	-288.4	5.26
		-416.6	7.17	-520.2	7.25	-281.9	4.39
	138	-405.1	5.45	-488.4	6.15	-283.2	4.28
		-384	4.5	-466.7	5.6	-291	5.45
		-406.3	7.23	-467.5	5.37	-282.2	4.25
		-421.2	8.66	-493	5.86	-282.3	3.84
7	150	-395.3	5.88	-466	5.77	-289.3	4.63
		-375	6.42	-444.8	6.77	-283.3	4.06
		-404.1	8.07	-444.2	6.29	-287.2	4.6
		-416.5	7.13	-460.1	5.88	-286	4.35
	162	-378.2	6.95	-423.5	5.69	-299.6	4.97
		-361.6	4.78	-405.3	6.06	-298.6	5.3
		-388.9	8.22	-403.6	5.31	-286.6	4.19
		-392.9	7.12	-421.6	5.42	-288.1	3.76

TABLE C5 Continued: MEASUREMENTS USING THE PR - MONITOR
AFTER 8 WEEKS

DRYING	TIME	FX - 228		MASTERFLOW -928		NO GROUT	
DAYS	HOURS	Ecorr	RATE	Ecorr	RATE	Ecorr	RATE
8	186	-365.9	6.51	-396.1	5.47	-299	4.2
	204	-375.5	5.8	-386.5	5.8	-298.3	4.73
		-345.6	5.59	-366.7	5.18	-305	5.12
		-389.8	6.9	-369.2	5.56	-293	4.16
		-368.2	6.95	-378.7	5.83	-300.6	5.44
9	216	-388.5	4.81	-391.9	5.62	-285.2	4.84
		-357	5.48	-368	5.18	-314.4	5.93
		-397.6	6.32	-378.1	5.14	-299.3	4.52
		-389.3	8.65	-378.9	5.75	-310.5	5.47
	228	-358.3	5.06	-378.2	5.62	-310.2	4.71
		-343.1	4.96	-376	5.76	-313.6	5.38
		-365	7	-389	5.52	-297.2	4.38
		-367.6	5.91	-385.1	6.62	-376.4	4.57
	240	-357.8	5.23	-354	5.4	-311.5	4.65
		-360.6	6.62	-362.9	5.45	-313.8	5.39
		-370.7	7.63	-356.8	5.46	-296.9	4.25
		-366.7	5.26	-389.1	6.61	-417.3	3.55

TABLE C6: AVERAGE OF READINGS
AFTER 8 WEEKS

DRYING TIME		FX - 228		MASTERFLOW -928		NO GROUT	
DAYS	HOURS	Ecorr	RATE	Ecorr	RATE	Ecorr	RATE
	0	-861.75	18.98	-957.95	19.78	-848.25	22.95
	6	-738.07	9.83	-921.68	12.55	-648.40	12.88
	18	-657.85	7.86	-765.18	9.47	-508.53	10.68
	24	-632.23	7.42	-718.73	9.90	-495.40	9.22
	30	-584.63	10.31	-710.27	23.51	-466.17	13.38
	42	-523.05	8.12	-666.65	9.87	-389.73	6.18
	48	-503.30	7.84	-673.18	7.20	-330.18	6.52
	54	-492.08	7.10	-666.63	7.63	-315.53	5.68
	66	-513.03	8.19	-641.80	8.70	-440.45	7.46
	78	-509.15	7.25	-612.60	7.61	-307.08	4.81
	90	-445.23	6.32	-594.65	7.39	-280.48	4.66
	102	-435.18	6.27	-556.40	6.87	-285.65	4.48
	114	-422.43	6.15	-526.18	6.99	-282.43	4.20
	126	-415.45	6.53	-505.23	6.47	-283.85	5.16
	138	-404.15	6.46	-478.90	5.75	-284.68	4.46
	150	-397.73	6.88	-453.78	6.18	-286.45	4.41
	162	-380.40	6.77	-413.50	5.62	-293.23	4.56
	186	-365.90	6.51	-396.10	5.47	-299.00	4.20
	204	-369.78	6.31	-375.28	5.59	-299.23	4.86
	216	-383.10	6.32	-379.23	5.42	-302.35	5.19
	228	-358.50	5.73	-382.08	5.88	-324.35	4.76
	240	-363.95	6.19	-365.70	5.73	-334.88	4.46

TABLE C7:MEASUREMENTS USING THE PR - MONITOR
AFTER 10 WEEKS (1HR SOAKING)

TIME		FX - 228		MASTERFLOW -9		NO GROUT	
DAYS	HOURS	Ecorr	RATE	Ecorr	RATE	Ecorr	RATE
1	0	-742.5	19.83	-822.9	31.22	-572.4	32.72
		-686.7	22.11	-876.7	19.84	-552.2	22.55
		-743.2	25.78	-836.8	20.73	-546.3	27.99
		-687.5	16.25	-846.4	26.9	-534.3	26.77
	12	-664.3	8.4	-866.6	13.62	-440.2	11.12
		-620.6	8.46	-774.5	10.66	-419.2	9.66
		-634.1	11.95	-768.8	12.7	-422.8	11.01
		-599.6	11.28	-807.2	14.64	-428.1	10.4
2	24	-529	7.63	-636.8	9.35	-344.5	5.76
		-512.8	6.3	-603.7	7.44	-343	6.8
		-501.1	8.94	-613.4	8.44	-342.4	5.93
		-517	8.59	-620.7	8.43	-326.4	5.03
	36	-496.7	5.86	-562.8	8.42	-339.3	5.47
		-481.8	6.45	-541	7.25	-338.7	5.7
		-477.6	10.36	-546.4	7.85	-336.5	5.65
		-486.8	7.14	-549.2	7.23	-328.9	5.82
3	48	-431.9	6.51	-476.6	6.19	-330.1	4.53
		-419.7	6.12	-462.9	6.5	-329	5.18
		-422.6	7.64	-466.8	6.43	-314.6	4.28
		-434.8	7.37	-457.2	7.09	-329.2	4.86
5	96	-357.2	6.96	-351.4	6.46	-334.1	4.59
		-349.8	5.78	-343	6.24	-333.1	5.31
		-357.1	7.41	-345.2	6.47	-336.5	4.86
		-355.3	6.22	-348.1	6.36	-340	4.33

TABLE C8: AVERAGES OF MEASUREMENTS IN TABLE C7

TIME	FX - 228		MASTERFLOW		NO GROUT	
HRS	Ecorr	RATE	Ecorr	RATE	Ecorr	RATE
0	-714.98	20.993	-845.7	24.673	-551.3	27.508
12	15.508	-824.99	18.789	-489.44	19.028	10.548
24	-514.98	7.865	-618.65	8.415	-339.08	5.88
36	-485.73	7.4525	-549.85	7.6875	-335.85	5.66
48	-427.25	6.7167	-465.88	6.5525	-325.73	4.7125
96	-354.85	6.5925	-346.93	6.3825	-335.93	4.7725

TABLE C9:MEASUREMENTS AFTER 13 WEEKS

TIME	FX			MASTERFLOW			NO GROUT		
(HOURS	Ecorr	Rs	Rate	Ecorr	Rs	Rate	Ecorr	Rs	Rate
1	-876.5	172	21.83	-946.2	224	22.78	-822.4	176	34.06
1	-868.7	215	28.55	-914.4	240	25.83	-793.9	211	31.39
1	-886.1	195	27.18	-919.2	244	23.88	-813.2	192	29.97
1	-886.1	195	27.18	-919.2	244	23.88	-813.2	192	29.97
24	-584.3	294	14.93	-632.5	401	9.41	-457.9	275	11.66
24	-604.4	229	8.82	-629.7	452	8.72	-436.9	332	12.33
24	-560.1	360	10.63	-616.4	367	6.41	-447.5	396	9.26
24	-562.2	364	12.08	-616.4	367	6.41	-486.1	305	12.18
36	-540.8	285	10.69	-571.6	359	7.89	-408.7	328	9.18
36	-524.7	226	6.11	-564.4	383	7.73	-405.6	404	8.12
36	-540.1	246	7.59	-560	346	7.76	-390.6	374	10.54
36	-509.4	295	8.92	-560	346	7.76	-390.6	374	10.54
48	-516.4	484	9.92	-548.5	385	8.8	-399.6	314	8.9
48	-486.3	242	6.85	-542.2	366	7.66	-439.2	271	7.47
48	-493.5	313	10.42	-541.1	374	7.44	-397.5	372	8.35
48	-519.4	269	9.11	-518.9	362	8.6	-479.6	258	6.16
60	-472	464	8.89	-494.8	432	7.55	-387.4	387	7.94
60	-437.1	358	8.16	-470.7	445	7.27	-366.2	458	8.93
60	-457.3	317	8.5	-491.7	444	8.11	-378.02	431	6.9
60	-482.1	280	9.04	-480.1	332	7.12	-409.7	375	6.25
84	-436	448	7.53	-427.2	559	6.81	-365.7	391	6.17
84	-414.3	493	9.64	-425.6	592	6.83	-354.1	432	7.71
84	-451.3	292	8.3	-420.5	474	7.84	-359.2	480	5.86
84	-417.4	332	7.23	-404.2	382	6.54	-370.3	485	5.13
108	-404.5	396	6.55	-401.5	610	7.58	-360.7	407	5.84
108	-386.4	451	7.72	-405.4	586	6.79	-352.2	473	7.53
108	-417.6	428	9.92	-397.7	430	6.04	-358.2	522	5.64
108	-403	425	8.07	-401.5	542	6.8	-357	468	6.34

TABLE C10:AVERAGE OF 13TH WEEK MEASUREMENTS

TIME		FX	MASTERFLOW		NO GROUT				
HRS	Ecorr	Rs	Rate	Ecorr	Rs	Rate	Ecorr	Rs	Rate
1	-879.35	194.25	26.185	-924.75	238	24.093	-810.68	192.75	31.348
24	-577.75	311.75	11.615	-623.75	396.75	7.7375	-457.1	327	11.358
36	-528.75	263	8.3275	-564	358.5	7.785	-398.88	370	9.595
48	-503.9	327	9.075	-537.68	371.75	8.125	-428.98	303.75	7.72
60	-462.125	354.75	8.6475	-484.33	413.25	7.5125	-385.33	412.75	7.505
84	-429.75	391.25	8.175	-419.38	501.75	7.005	-362.33	447	6.2175
108	-402.833	425	8.0633	-401.53	542	6.8033	-357.03	467.33	6.3367

TABLE C11: MEASUREMENTS USING THE RPX1
AFTER 4 WEEKS

	Ecorr Measurements (RPXI)		
TIME(HR	FX	MF	NG
0	-1105	-1097	-990
	-1047	-878	-930
	-1047	-879	-918
		-958	-897
4	-935	-974	-1127
	-934	-973	-1127
	-936	-978	-1126
	-936	-875	-1111
8	-994	-917	-992
	-993	-907	-992
	-929	-1039	-993
	-928	-1039	-993
12	-1005	-906	-996
	-1005	-907	-995
	-983	-1039	-1074
	-982	-1039	-1073
24	-1064	-1011	-996
	-942	-892	-995
	-1027	-891	-1074
	-1027	-900	-1073

TABLE C12: AVERAGE MEASUREMENTS

	Ecorr Measurements (RPXI)		
TIME(HR	FX	MF	NG
0	-1066.3	-953	-933.75
4	-935.25	-950	-1122.8
8	-961	-975.5	-992.5
12	-993.75	-972.75	-1034.5
24	-1015	-923.5	-1034.5

TABLE C13: MEASUREMENTS USING THE RPX1 AFTER 6 WEEKS

	Ecorr Measurements (RPX1)		
TIME(HRS)	FX	MF	NG
0	-836	-935	-849
	-833	-936	-853
	-834	-903	-833
	-835	-927	-828
6	-739	-884	-650
	-737	-845	-646
	-743	-871	-631
	-720	-849	-653
12			
18	-622	-722	-431
	-623	-720	-483
	-635	-695	-444
	-628	-696	-440
24	-634	-686	-378.6
	-616	-696	-406
	-625	-671	-401
	-628	-663	-382.3
30	-589	-673	-424
	-606	-659	-440
		-643	-436

TABLE C14: AVERAGES OF TABLE C13

	Ecorr Measurements (RPX1)		
TIME(HRS)	FX	MF	NG
0	-834.5	-925.25	-840.75
6	-734.75	-862.25	-645
18	-627	-708.25	-449.5
24	-625.75	-679	-391.975
30	-597.5	-658.333	-433.333

APPENDIX D
CORROSION RATE PLOTS

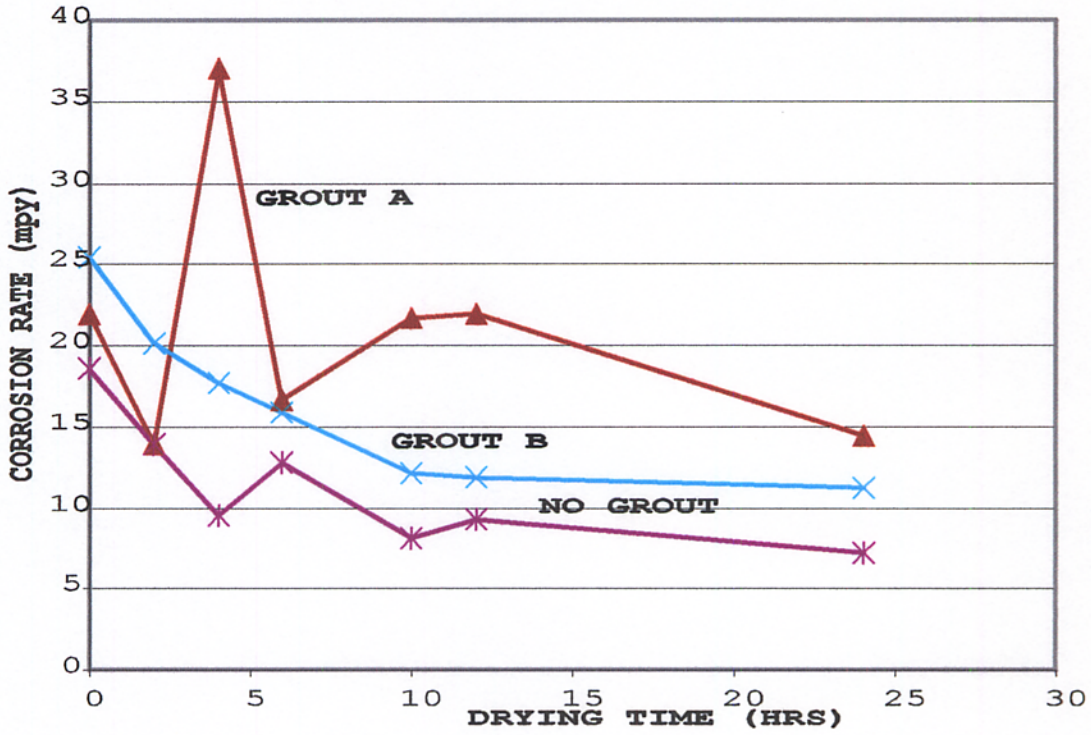

Figure D1 : Corrosion Rate Vs. Drying Time After 2 Weeks.

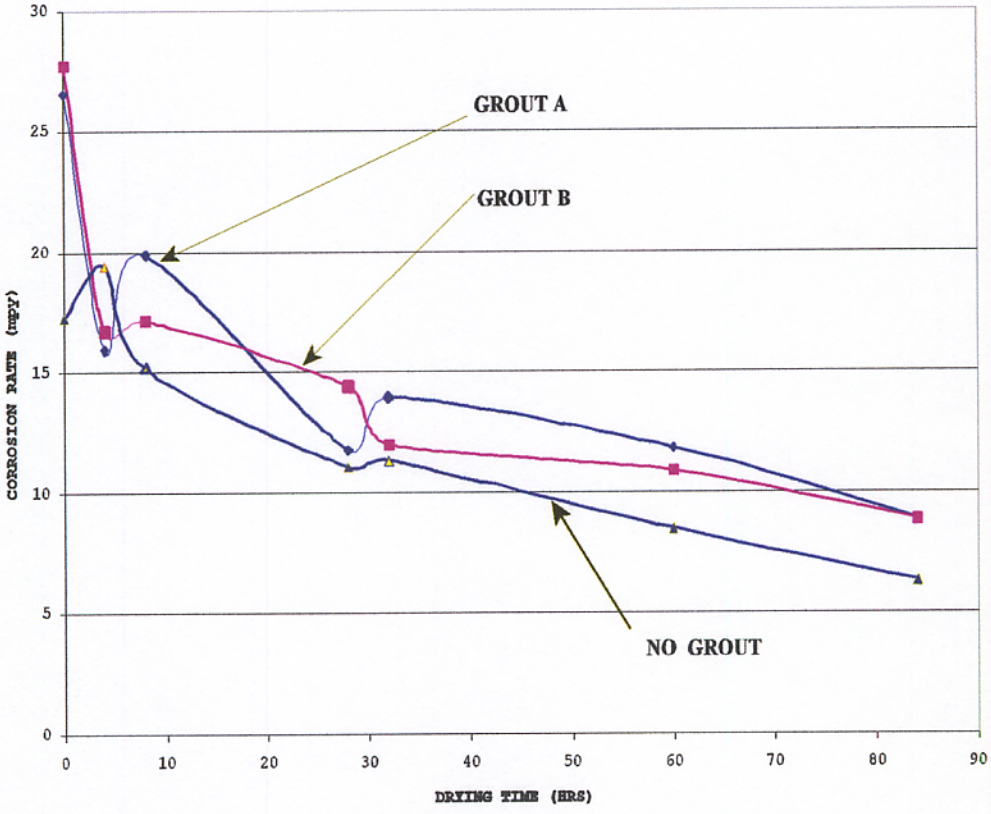

FIGURE D2: Corrosion Rate Vs. Drying Time After 4 Weeks.

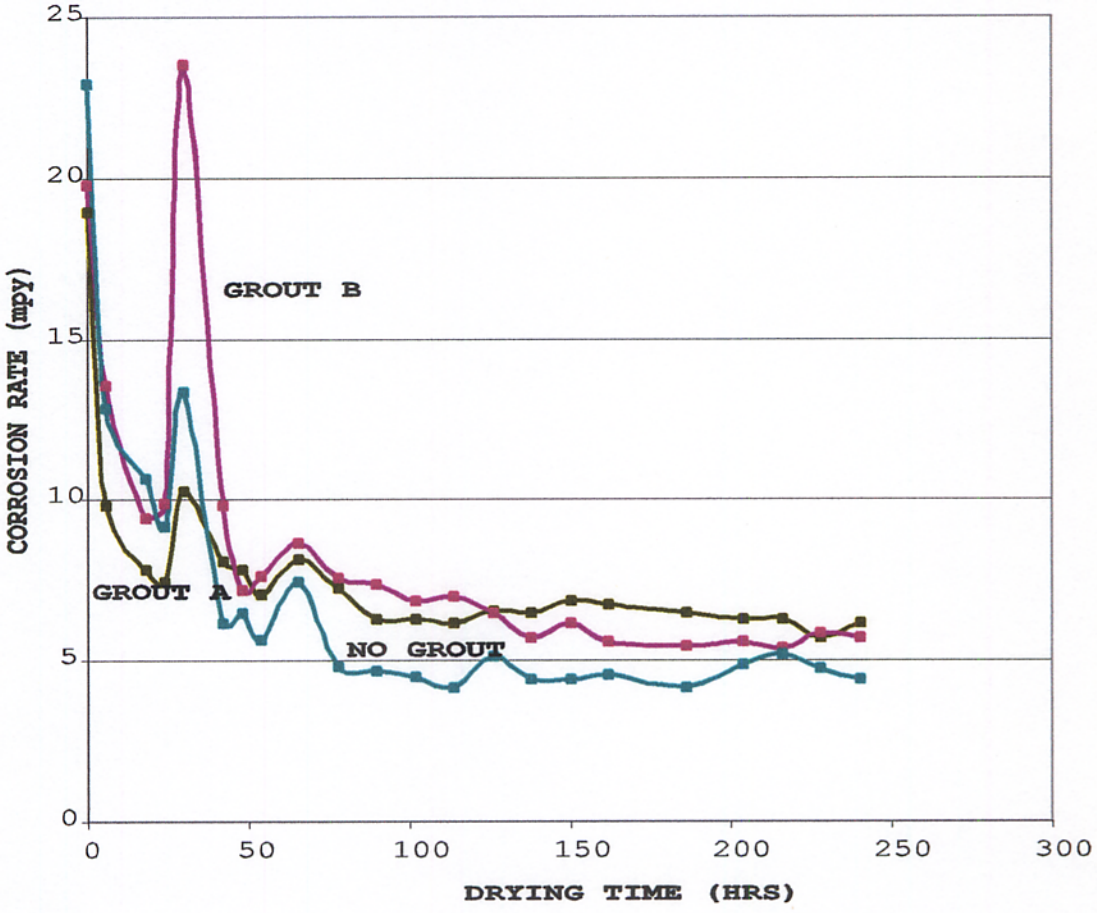

Figure D3: Corrosion Rate Vs. Drying Time After 8 Weeks

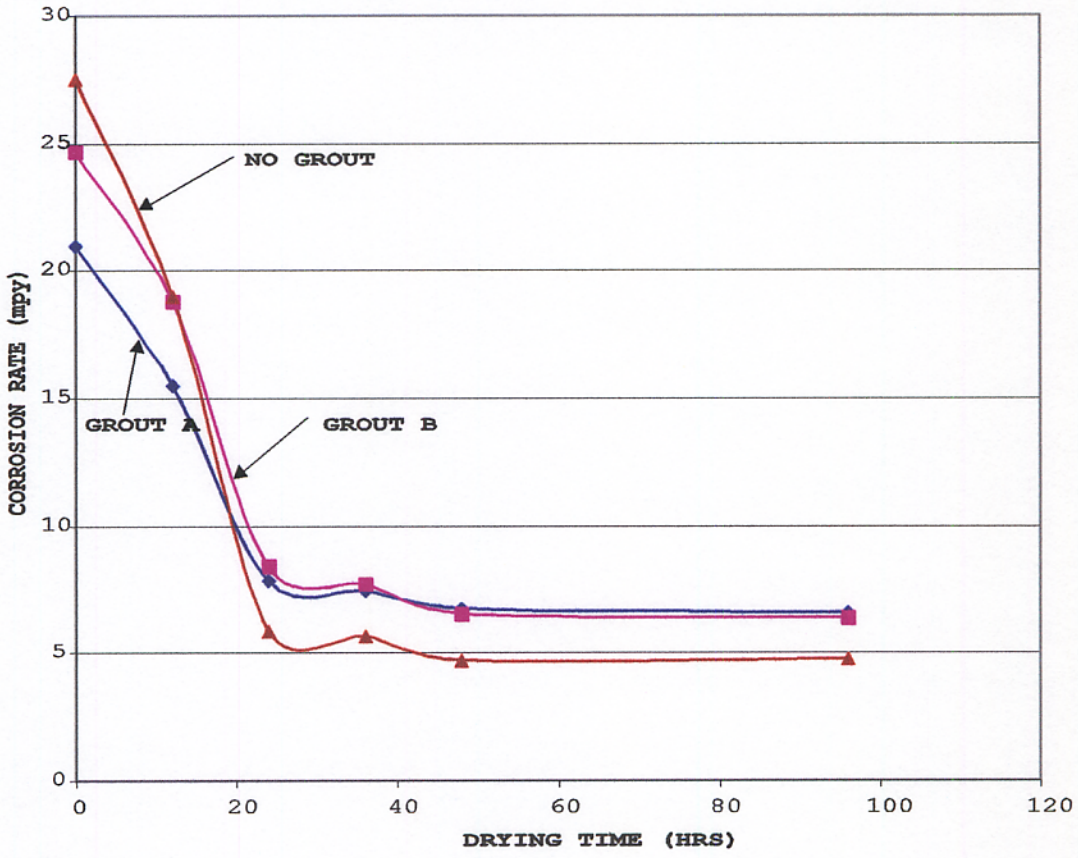

Figure D4 : Corrosion Rate Vs. Drying Time After 10 weeks (1 hr. Soaking)

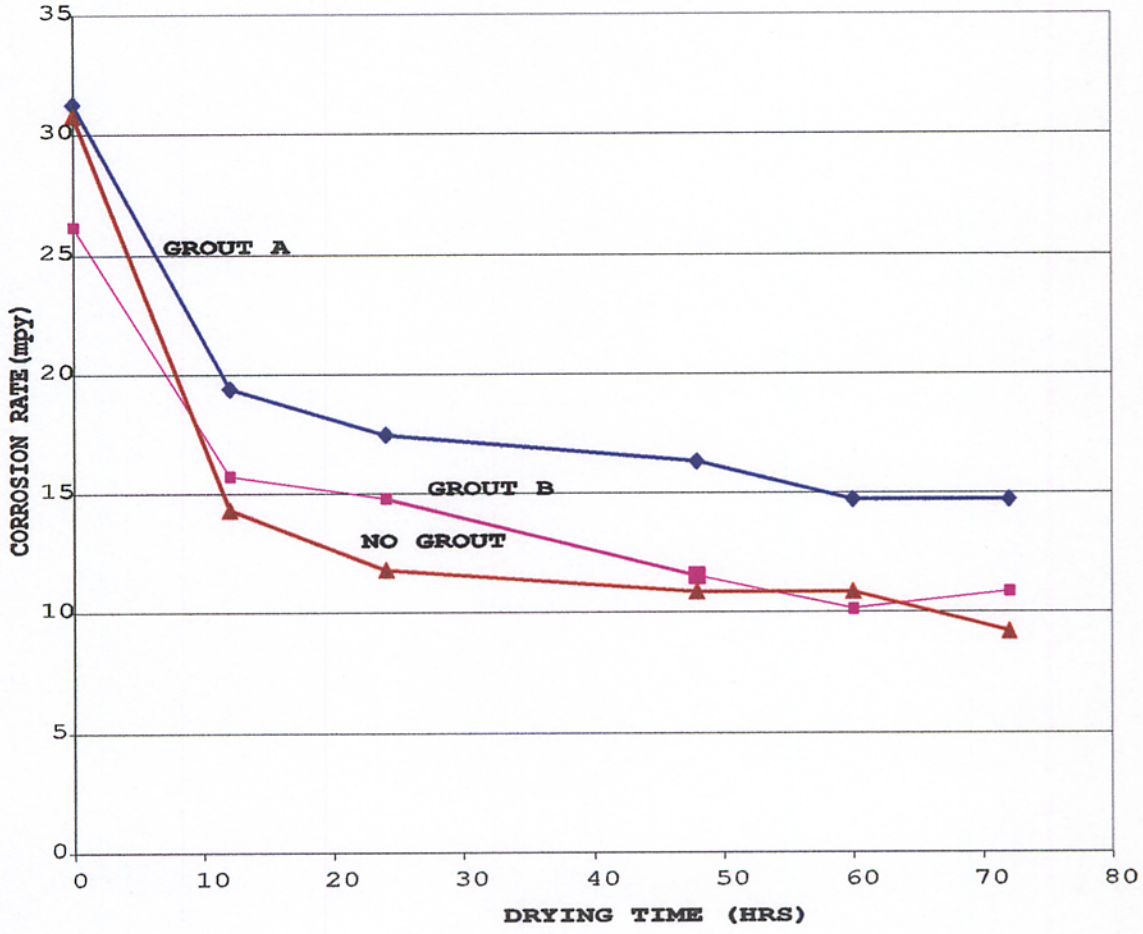

Figure D5 : Corrosion Rate Vs. Drying Time After 11 Weeks (30 minutes soaking)

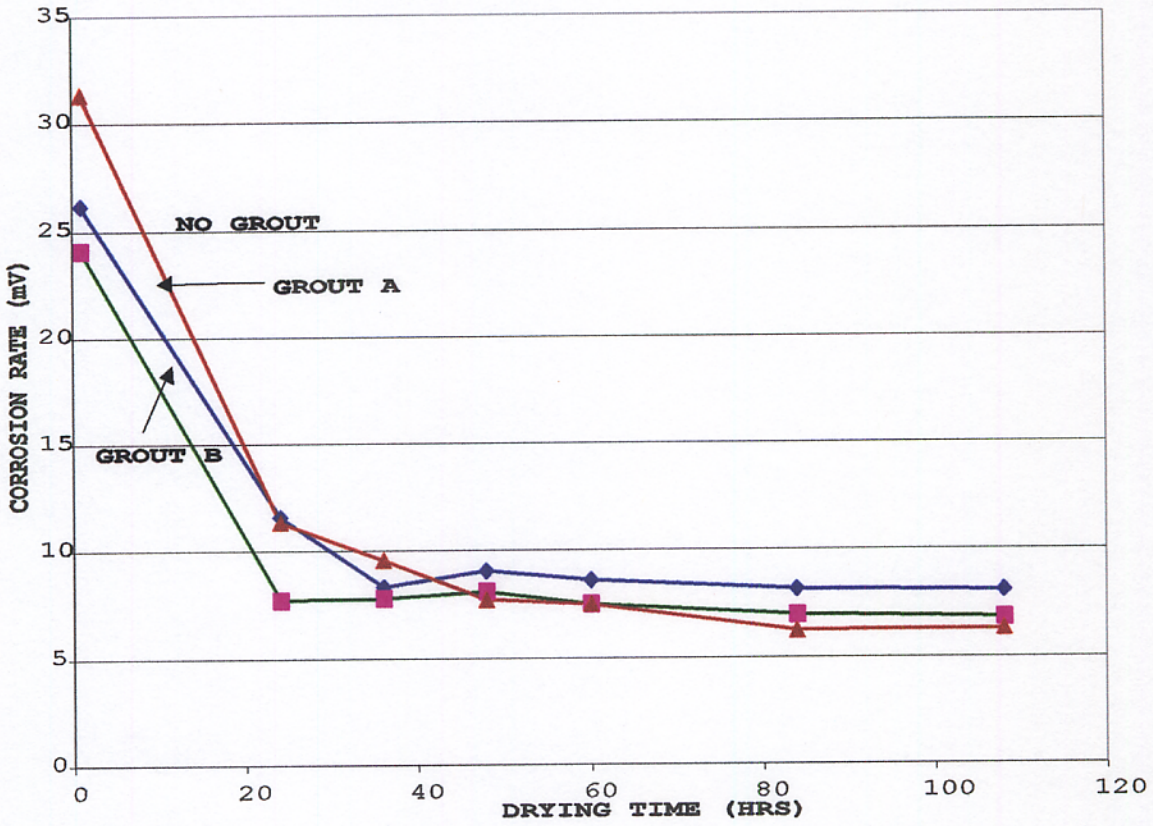

Figure D6 : Corrosion Rate Vs. Drying Time After 13 Weeks

REFERENCES

1. McCarter, W. J., Monitoring the Influence of Water and Ionic Ingress on Cover-Zone Concrete Subjected to Repeated Absorption. Cement, Concrete and Aggregates, CCAGDP, Vol. 18 No. 1 June 1996, pp 55 - 63.

2. Cook, R.A., Nieporentt, S.B, and Ansley, M.H., Deflection Calculation Model for Structures with Annular Base Plates. Research report for Engineering and Industrial Experiment Station, University of Florida, Gainesville Florida, 1997.

3. Cook, R.A., Ellifritt S. D., Schmidt E. S., Adediran A., andBeese W. Design Procedures for Annular Base Plates. Research report No. 95-4 Engineering and Industrial Experiment Station, University of Florida, Gainesville Florida, 1997.

4. Akthem A.,Al-Manaseer and L.Douglas Keil , Physical Properties of Cement Grouts Containing Silica Fume and Superplasticizer. ACI Materials Journal, March - April, 1992. PP 154 - 160

5. Hausemann D. A . Steel Protection in Concrete, how does it Occur. Material Science Vol. 6, 1967. PP 19 - 23

6. Papadakis V. G.,Fardis M. N. and Vayenas C. G. Materials and Structures, Vol. 21, No.149 (1992). Effect of composition, environmental factors and cement-lime mortar coating on concrete carbonation. PP 293 -304.

7. Lars-Olof Nilson and Tang Luping. Rilem Report 12,1995 pp 15 - 32: Relations between different Transport modes.

8. Mang Tia, David Bloomquist, Yang M. C. K., Meletiou, C. A., Amornsrivilae, P., Shih, C., Bobson, E., and Richardson, D. Extension Study of Modulus of Rupture and Permeability of Structural Concrete in Florida for Development of a Concrete Performance Specifications. Research report NoFL/DOT/RMC/0384-3366 Engineering and Industrial Experiment Station, University of Florida, Gainesville Florida, 1992

9. Hall C.(1989) Water Sorptivity of Mortars and Concretes, a Review. Magazine of Concrete Research, Vol. 41, No. 147,pp.51 - 61.

10. Mette Geiker, Horst Grube, Tang Luping, Lars- Olof Nilson and Carmen Andrade. Laboratory Test Methods. (RILEM REPORT, 1995, Edited by J.Kropp and H. K. Hilsdorf (Performance Criteria for Concrete Durability) pp 213 - 257.

11. Page C. L.Basic Principles of Corrosion. (RILEM REPORT, 1988, Edited by P. Schiessl (Corrosion of Steel in Concrete)), pp 3 - 21.

12. Figgs J.W. (1973) Methods of Measuring the Air and Water Permeability of Concrete. Magazine of Concrete Research, Vol. 25 No. 85 pp213 - 219.

13. Lopez W. and Gonzalez J. A. Influnce of the Degree of Pore Saturation on the Restitivity of Concrete and the Corrosion Rate of Steel Reinforcement.Cement and Concrete Research,Vol. 23 pp. 368 - 376, 1993.

14. C. Andrade (1988) Monitoring Techniques. RILEM Report on Corrosion of Steel in Concrete (1988) Edited by P. Schiessl. pp 79 - 95.

15. Stern, M.S. and Geary, A. J. Journal of the Electrochemical Society, Vol. 104,1957, pp. 56.

16. Feliu, S., Gonzalez, J. A., Andrade, C., and Feliu, V. Corrosion NACE paper No. 145 San Francisco, March 1987.

17. Gonzalez, J.A, Algaba, S., and Andrade C., Corrosion of Reinforced Bars in Carbonated Concrete. British Corrosion Journal. Vol.15 (1980) pp. 135-139.

18. Broomfield, J. P., Rodriguez, J Ortega, L. M. and Garcia, A. M. Corrosion Rate Measurements and Life Prediction for Reinforced Concrete Structures, Proceedings of Structural Faults and Repair -1993, Vol2,pp.155-164

19. 1997 Annual Book of ASTM Standards, Parts10 and 14.

20. G. C. Kostogloudis. Comparative Investigation of Corrosion Resistance of Steel Reinforcement in Alinite and Portland Cement Concrete. Cement and Concrete Research, Vol. 28. No. 7, pp 995 - 1010, 1998.

21. Wrobel P., Laboratory Measurement of Corrosion Activity of Steel Reinforcement in Concrete Using Simple Equipment, Cement, Concrete and Aggregates, CCAGPD, Vol. 16, No. 2, Dec, 1994, pp 100 - 103.

22. G. Batis, N. Couloumbi and A. Katsiamboulas., Durability of Reinforced Lightweight Mortars with Corrosion Inhibitors. Cement, Concrete and Aggregates, CCAGDP,

Vol. 18, No. 2, 1996, pp. 118 - 125.

23. Syed Ehtesham Hussain and Rasheeduzzafar, Corrosion Resistance Performance of Fly Ash Blended Cement Concrete. ACI Materials Journal, May - June 1994, pp 264 -271.

24. N. Gowripalan and H. M. Mohammed, Chloride - Ion Induced Corrosion of Galvanized and Ordinary Steel Reinforcement In High-Performance Concrete. Cement and Concrete Research, Vol.28, No. 8, pp 1119 - 1131, 1998.

25. Zhang, X. G. and Valeriote, E. M.., Galvanized Protection of Zinc Under Thin Layer Electrolytes. Atmospheric Corrosion, ASTM STP 1239, W. W. Kirk and Herbert H. Lawson, Eds., American Society for Testing and Materials, Philadelphia, 1995.

26. Gonzalez, J. A, and Molina A., Errors in the Electrochemical Evaluation of very small Corrosion Rates - II. Other Electrochemical Techniques Applied to Corrosion of Steel in Concrete. British Corrosion Journal, Vol.15, No. 138 1980.

27. Andrade C, and Gonzalez J. A. Quantitative Measurements of Corrosion of Reinforcing Steels Embedded in Concrete Using Polarization Resistance Measurements. Werkst Korros, Vol. 29, No. 515 1978.